SAPIENZA
Università di Roma
Facoltà di Scienze Matematiche Fisiche e Naturali

DOTTORATO DI RICERCA
IN GENETICA E BIOLOGIA MOLECOLARE

XXXIV Ciclo
(A.A. 2021/2022)

Common Fragile Sites: a new tool to study chromosome instability diseases

Dottoranda
Elisa Balzano

Docente guida
Prof.ssa Franca Pelliccia

Tutore
Prof. Antonio Antoccia
Prof.ssa Simona Giunta

Coordinatore
Prof. Fulvio Cruciani

INDEX

GLOSSARY

Chromosomal Fragile Sites: Large chromosomal regions prone to gaps and breaks

Fanconi Anemia: A rare inherited disease caused by mutations in any of 22 genes, characterized by bone marrow failure, multiple congenital abnormalities and cancer predisposition

Glioblastoma Multiforme: Fast-growing and aggressive brain tumor (astrocytoma grade IV), resistant to therapy

Chromosomal Instability: Increased rate of changes in both chromosome numbers and structure

Chromothripsis: Massive localized chromosomal rearrangement in response to a single catastrophic event that results in chromosome shattering

Chromosomal Instability disease: Group of disorders associated with chromosomal instability and breakage either spontaneously or in response to DNA damaging agents

ABSTRACT

Replication stress is a major cause of Chromosomal Instability (CIN) that manifests as chromosome rearrangements, gaps and breaks, including those cytological expressed within specific chromosome regions named Common Fragile Sites (CFSs). The molecular mechanisms of CFSs instability have not been completely elucidated yet. In the first part of my work, I characterized the expression and the replication timing of human CFSs upon treatment with aphidicolin (APH), a DNA polymerase α (alpha) inhibitor, in three cellular lines: Glioblastoma Multiforme U-251 MG cell line and two isogenic Fanconi Anemia lymphoblastoid lines (the mutated HSC72 FA-A and the corrected HSC72 FANCA). GBM and FA cell lines are both associated with high physiological levels of CIN and thus are good genetic models to understand the causes underlying CFSs instability. Glioblastoma Multiforme (GBM) is a tumor of the Central Nervous System (CNS) and Fanconi Anemia (FA) is a rare multigenic disorder caused by mutations in FA DNA repair genes. I identified CFSs that showed a frequency equal to at least 1% of the total gaps/breaks: 17 CFSs in GBM, 16 CFSs in HSC72 FA-A, 19 CFSs in HSC72 FANCA. Only few of them were found to be cell type-specific. In the last part of my work, CFSs induced by 4', 6′-diamidino-2-phenylindole hydrochloride (DAPI), a DNA dye binding to AT-rich sequences and acting as an under-condensing agent in G2-phase, were analyzed in a pathological background such as FA cells (which are characterized by a prolonged G2-phase upon DNA damage) to understand how the post-replicative chromatin compaction is essential to their integrity. Presence of long genes, incomplete replication, improper chromatin condensation and DNA synthesis during mitosis (MiDAS) after APH and DAPI treatment suggest that impaired replication process and defective chromatin compaction may contribute to the loci-specific fragility in U-251 MG cells and in both HSC72 FA lymphoblasts cell lines. Altogether, my work offers a comprehensive characterization of CFSs expressed in GBM and FA cells that may be further exploited for cytogenetic and clinical studies to advance our understanding of the physiological status and these genic and genetic disorders.

INTRODUCTION

History of Chromosomal Fragile Sites

Fragile Sites (FSs) are chromosomal regions that appear as structural aberrations, such as gaps and breaks with a frequency equal to at least 1% of the total number of chromosome lesions (Le Tallec et al., 2011,Le Tallec et al., 2013, Miron et al., 2015). In 1965, Dekaban observed for the first time the recurrence of a FS on chromosome 9 in lymphocytes metaphases obtained from peripheral blood of women with eczematous dermatitis (Dekaban, 1965). Following studies showed that the culture conditions - including lack of folic acid and thymidine in the cell culture medium (Sutherland, 1977) - contributed to the expression of such breaks (Sutherland, 1979). In the early 80s, Glover and colleagues showed for the first time the induction of DNA lesions in specific chromosomal regions by using aphidicolin (APH), a DNA polymerase α (alpha) inhibitor (Glover, 1984).
Although more than 200 FSs have been identified so far in the human genome and appropriately annotated on the NCBI Genome Database (Mrasek et al, 2010), only few of them have been molecularly characterized.

Classification of Chromosomal Fragile Sites

The characterization of chromosomal fragile sites is in constant evolution. The complexity of studying chromosomal fragile sites is due to their variable cytological expression. Their expression frequency on metaphase chromosomes depends on different factors, including the type of chemical inducer and its concentration in a particular cellular background. The criteria used for the classification of FSs are frequency, hereditability within the population and mode of induction, as defined during the Helsinki Conference on Human Gene Mapping in 1985 (Berger et al. 1985). Based on these criteria, two main classes of FSs exist: Rare and Common.

Rare Fragile Sites (**RFSs**) are expressed in the cell population at a frequency of less than 5%. RFSs are also defined as heritable fragile sites because they segregate according to the Mendelian laws. The peculiarity of RFSs is the repetitiveness of di/tri-nucleotides, which have the potential to form DNA secondary structures and therefore affect replication fork progression (Schwartz et al., 2006). Their cytological expression is due to the progressive expansion of these repeated sequences. The best-known clinical example is the FRAXA folate sensitive RFS (Xq27.3), in which the triplet CGG amplification at the 5 'UTR of the FMR1 gene causes the lack of the FMRP protein (fragile X mental retardation protein), necessary for both a correct cognitive development and gametogenesis (Martin and Bell, 1943; Tassone et al., 2003).

Contrary to the polymorphic RFSs, **Common Fragile Sites** (**CFSs**) are not composed of repeat-rich sequences. CFSs owe their name to the frequency with which they occur in the population. In fact, CFS loci are present in the cells of all analyzed individuals and they are constitutional present in the chromosomes. Most CFSs are elicited by aphidicolin (APH), a DNA polymerase α (alpha) inhibitor.
FRA3B (3p14.2) stands out like the most Fragile Site in the human genome, indeed it can be cytologically induced in the majority of cell types (Le Beau et al., 1998).
Interestingly, this fragile chromosomal locus is conserved as ortholog of human FRA3B in murine species (Fra14a2) (Shiraishi et al., 2001). Although the molecular mechanisms underlying their instability are still unclear, replication process impairment seems to have a major role in CFSs induction (Glover et al., 2005; Schwartz et al., 2006) (Figure 1).

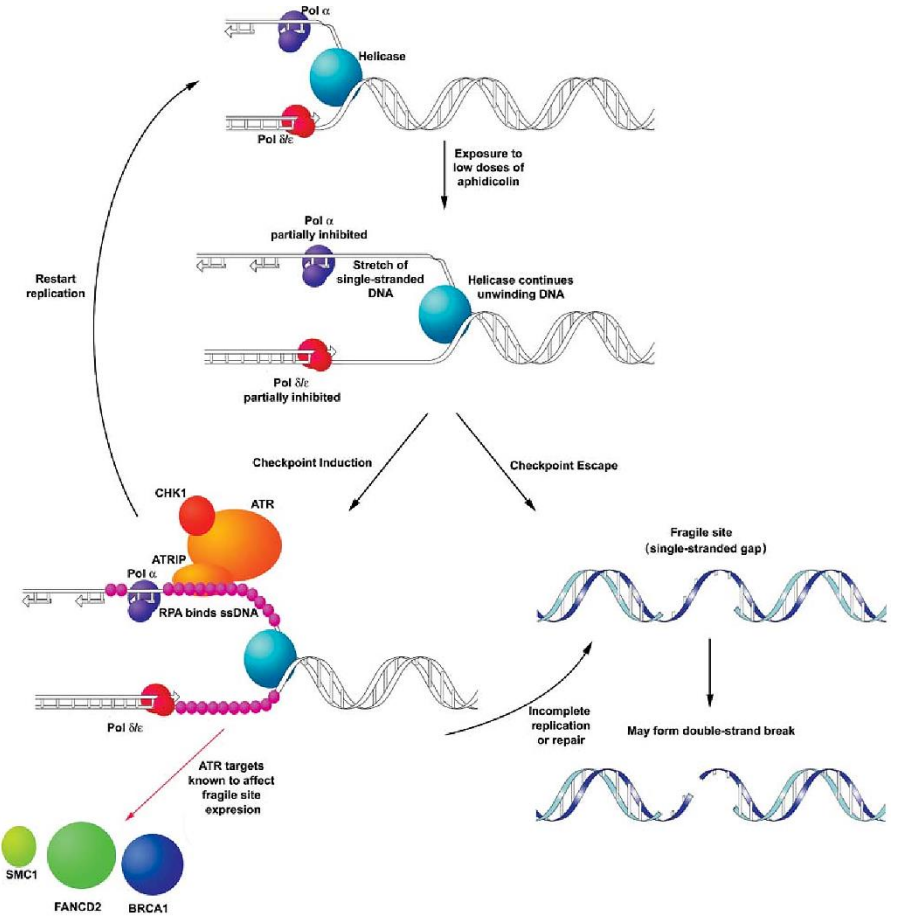

Figure 1. Suggested model for instability at CFSs. The single-stranded DNA (ssDNA) at delayed or stalling replication fork recruits the DNA binding protein RPA (Replication Protein A), leading to the activation of the S-phase and/or G2/M checkpoints (ATR pathway). ATR/ATRIP (Ataxia-Telangiectasia mutated and Rad3-related/ATR-interacting protein) complex recruits BRCA1 (Breast Cancer Type 1 Susceptibility Protein), FANCD2 (FA Complementation Group D2) and SMC1A (Structural maintenance of chromosomes protein 1A) for the replication fork maintenance. When the lesion (Single Strand Break, SSB) escapes from the checkpoint control, a Fragile Site manifests on metaphase chromosomes; if the SSB is not repaired, it can lead to DSB (Double Strand Break) (Glover et al., 2005).

Common Fragile Sites (CFSs)

CFSs have been defined as late replicating regions in which late and incomplete replication leads to breakage or defective chromatin condensation (Durkin and Glover, 2007). CFSs are not caused by a single factor, but rather by a combination of different mechanisms (Franchitto, 2013). Although several studies have attempted to identify such mechanisms (Zlotorynski et al, 2003; Durkin and Glover, 2007), the exact contribution of CFSs molecular features in the replication process impairment remains unknown.
Except for being relatively enriched in AT sequences, CFSs do not share any specific sequences. Despite the nucleotide composition of CFSs does not provide immediate clues to their instability, these sequences can potentially form flexible secondary structures. Alternative DNA conformations, such as secondary structures, can hinder DNA polymerase progression and, hence, they are detrimental for a complete replication process (Lukusa and Fryns, 2008).
A new class of DAPI-inducible CFSs demonstrated how critical is the configuration of these AT-rich sequences for their integrity (Pelliccia and Rocchi, 1986). In fact, DAPI (4′,6′-diamidino-2-phenylindole hydrochloride) can act as an under-condensing agent that binds specifically the AT-rich sequences in the minor groove of the DNA double helix (Kapuscinski and Szer, 1979; Prantera et al., 1981; Portugal and Waring, 1988; Jeppesen and Nielsen, 1989).
Moreover, CFSs are chromatin regions with a defective condensin loading potentially due to an under-replicated state which persists until mitosis. These faulty chromatin-folding regions have been identified as sites of mitotic DNA synthesis (MiDAS) (Boteva et al., 2020) as observed by using the mitotic incorporation of the analog of thymidine EdU (5-Ethynyl-2′-deoxyuridine) (Bergoglio et al., 2013; Minocherhomji et al, 2015; Macheret et al., 2020; Ji et al., 2020). Further evidence reported the colocalization of proteins required for MiDAS with CFS sites, such as FANCD2 (Naim et al., 2009; Madireddy et al., 2016; Macheret et al., 2020), RAD51 (DNA Repair Protein RAD51 Homolog 1) and MUS81-EME1 (MUS81 Structure-Specific Endonuclease Subunit-Essential Meiotic Structure-Specific Endonuclease 1) (Naim et al., 2013; Bhowmick et al., 2016).

In conclusion, CFSs are chromosomal sites of greater susceptibility to replicative stress and their cytogenetic localization depends also on the tissue and the cell differentiation status.

What shapes the cell type-specificity of CFSs?

Growing evidence has shown that CFSs instability can vary between different cell types in response to replicative stress conditions, suggesting that the maintenance of genomic stability has a complex nature (Debatisse et al., 2012).
Although FSs have been studied and mapped mainly in lymphocytes, they are expressed in all cell types, albeit with different frequencies (Debatisse et al, 2012).
Many CFSs present in lymphocytes harbor genes longer than 650 kb, called very long genes (VLG) (Smith et al, 2006; Bosco et al, 2010). A direct connection has been suggested between the long gene transcription and the instability level of the corresponding region (Brison et al, 2019). The transcription of human genes larger than 800 kb takes over more than one cell cycle, leading to an inevitable collision between replication and transcription machineries with the formation of DNA-RNA hybrids (R-loops) (Helmrich et al, 2011). Low transcription level of these long genes can be more harmful than high transcription level. Indeed, CFSs colocalize with long, low transcribed and late-replicating genes (Blin et al, 2018)
It has also been recently shown that APH delays replication timing (RT) of actively transcribed long genes in both fragile and non-fragile loci, highlighting that delayed replication timing and transcription processes are not sufficient to drive CFSs fragility but rather their chromatin conformation determines fragility (Sarni et al., 2020). The higher-order chromatin structure modulates several cellular processes, including gene expression and cell identity (Hiratani and Gilbert, 2009). Sub-nuclear domains epigenetically establish the activation of replication origins and presumably for this reason CFSs exhibit tissue-specific expression (Sarni et al., 2020).
DNA replication is a temporarily- and spatially-orchestrated process, and its alterations can affect the whole genome stability. The number and position of active replication origins (ORI) seem to be decisive for

the late CFSs replication timing and its expression. Replication analysis on FRA3B, the most known CFS, demonstrated a different program of initiation events between human lymphocytes and fibroblasts (Letessieret al., 2011; Debatisse et al., 2012).
In lymphocytes, the *core* of the FS is "poor" in fired replication origins and the few "long-traveling forks" converge late in S-phase or in G2-phase. When these "long-traveling forks" undergo APH replicative stress, the result is an incomplete replication (Figure 2A, left panel).
In fibroblasts, on the other hand, the replication dynamics is completely different due to the several initiation events inside the *core* of fragility.
This different ORI licensing appears more evident under replicative stress, where the slowing of the replication forks is compensated by an increase in the origins density (called flexible or dormant origins), resulting in the completion of replication before the M phase (Figure 2A, right panel).
The plasticity of spatial-temporal pattern of active ORI establishes the CFS replication profile and so its expression frequency. Indeed, FRA3B is expressed with a higher frequency in lymphocytes than in fibroblasts (Figure 2B).

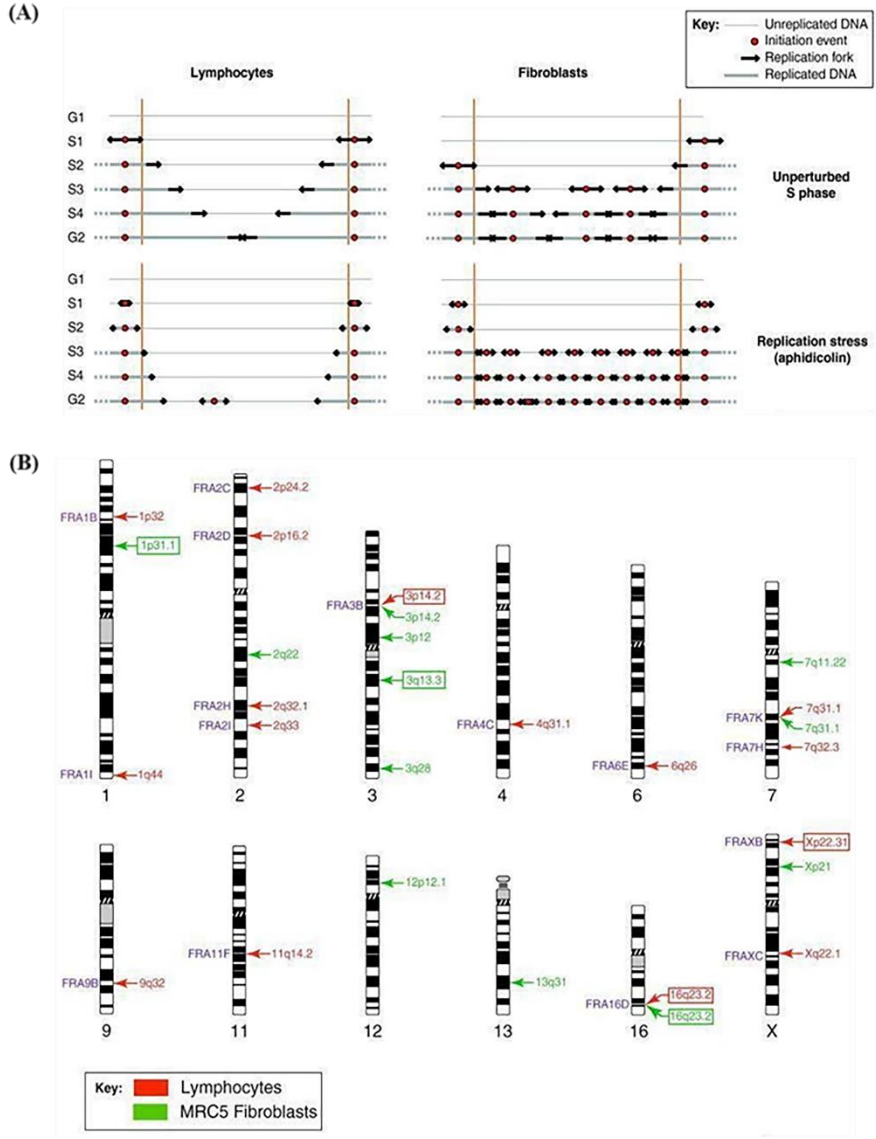

Figure 2. Schematic representation of replication timing of FRA3B region in human lymphocytes and fibroblasts in unperturbed and APH-stressful conditions. The *core* region is delimited by orange lines; cell cycle phases are represented on the left (A). Localization of Common Fragile Sites on human chromosomes of lymphocytes (red) and fibroblasts (green). CFSs with an expression frequency greater than 1.5% are shown. In brackets, the most expressed CFSs in each cell type are indicated (B). Modified from Debatisse et al., 2012.

CFSs as clinical tools for Chromosomal Instability disorders

Chromosome Instability (CIN) is the hallmark of cancer as well as genetic diseases, and CFS are the preferential loci in which instability occurs.
CFSs are the primary vulnerable sites of the genome under partial inhibition of DNA synthesis (Li and Wu, 2020), and CFSs-related chromosome aberrations can lead to aberrant chromosome rearrangements, becoming a source of both s-CIN (structural-CIN) and n-CIN (numerical-CIN) (Mitelman et al., 1997; Chan et al., 2009; Wilhelm et al., 2020).
This type of chromosome and genome reorganization can reset entirely the cell transcriptome. If the fragile chromosomal region holds genome guardian genes such as proto-oncogenes or tumor suppressor genes, it could represent a step towards initiation of cancer progression with an unregulated proliferation and an accumulation of mutations (Li et al., 2020; Simpson et al., 2021).
Additionally, CFSs are involved in breakage-fusion-bridge (BFB) cycles, giving rise to intra-chromosomal genic amplification (Hellman et al., 2002; Pelliccia et al., 2010).
FRA3B (3p14.2) was the first characterized cancer-related FS.
This FS contains the tumor suppressor gene Fragile Histidine Triad Diadenosine Triphosphatase (FHIT), a target of chromosome rearrangements in different types of cancer (Huebner et al, 1998).
The identification of the molecular basis of CIN is challenging and mapping these non-random fragile loci throughout the human genome could be exploited to detect specific replication stress-sites and, hence, to understand the pathogenetic mechanisms involved in the onset of chromosomal instability syndrome such as Fanconi Anemia, Ataxia-telangiectasia, Bloom syndrome, Seckel syndrome, Nijmegen breakage syndrome or also cancer (Taylor, et al., 2019).

AIM OF THE RESEARCH

CFSs are known to be hotspot sites for chromosome aberrations and are critical elements in promoting genomic instability in human diseases. The molecular features involved in their expression are not completely known yet.
The principal aim of my study was therefore to investigate the relationship between replication stress and cytogenetic expression of CFSs and analyze how CFSs can impact in both structural and numerical CIN.
To this purpose, I examined the effect of a mild replication stress (APH treatment) in two different complex clinical models of Glioblastoma Multiforme (GBM) and Fanconi Anemia (FA).
Glioblastoma is a tumor of the Central Nervous System (CNS) that is resistant to therapy because of high level of CIN and mis-regulated DNA repair; GBM cells suffer oncogene-induced replicative stress that synergizes with the occurrence of mitotic errors to trigger gross chromosomal rearrangements such as chromothripsis events (Cortés-Ciriano et al., 2020; Li et al., 2020).
Fanconi Anemia is a CIN-related syndrome featuring an altered FA pathway, essential for the DNA repair during the replication process and therefore this mutated FA pathway generates a delay of the cell cycle. About 60 to 70% of the FA patients shown mutations in FANCA gene (Buchwald, 1995).
FA patients present pancytopenia (decreased number of blood cells) with multiple congenital abnormalities and cancer predisposition (Nalepa et al., 2018).
For my studies, I used the GBM U-251 MG cell line and two isogenic FA lymphoblastoid cell lines derived from the same FA patient: HSC72 FANC-A cell line mutated in FANCA gene and HSC72 FANCA cell line corrected for the FANCA gene.
The use of isogenic cell lines allowed me to assess the differences specifically related to defects in the FANCA gene.
In addition, an important part of my work was dedicated to the characterization of a particular class of fragile sites induced by DAPI (4',6′-diamidino-2-phenylindole hydrochloride) in the two isogenic FA lymphoblastoid cell lines.

DAPI acts as under-condensing agent for AT-rich sequences in G2-phase and studying its effect in FA pathological background (prolonged G2-phase upon DNA damage) could clarify the importance of post-replicative processes (S/G2-phase transition), such as chromatin condensation, in the maintenance of CFSs integrity. Open chromatin promotes DDR (DNA Damage Response) in response to DNA damage, coordinating the DNA damage signal and recruitment of the DNA repair factors (Smerdon, 1991; Soria et al., 2013)

As control, lymphocytes taken from peripheral blood of healthy individuals were used to examine the effects of both APH and DAPI treatments. Fibroblasts previously used in Maccaroni et al., 2020 were also compared with these cell lines to further analyze the tissue-specific responses to APH stress condition.

In the first part of my work, I performed detailed cytogenetic observations of nuclei/chromosomal aberrations and cytological characterization of metaphase gaps and breakages expressed with a frequency higher than 1% of the total number of gaps/breaks. To specify the connection of chromosomal lesions with the presence of active transcribed genes, I then analyzed the molecular sequence of the cell-type specific CFSs.

In the second part of my work, I investigated the relationship between DNA replication and fragility of CFSs by analyzing the replication timing of the most expressed CFSs in every cell line, using combined FISH-IF against-BrdU (5-Bromo-2'-deoxyuridine) on interphase nuclei.

RESULTS AND DISCUSSION

Characterization of CIN under replication stress in Glioblastoma Multiforme and Fanconi Anemia cells

To understand how replication stress affects GBM cells and FA cells proliferation, the mitotic index (M.I.) was evaluated in the GBM U-251 MG cell line as well as in two isogenic lines of FA lymphoblasts compared with primary lymphocytes and MRC-5 fibroblasts upon treatment with low dose aphidicolin (APH 0.4 μM) for 24 hrs.
The percentage of mitotic cells on the total number of cells (N=500) was significantly reduced in lymphocytes, U-251 MG cells and corrected HSC72 FANCA lymphoblasts upon APH treatment compared to their untreated counterpart (Figure 3).

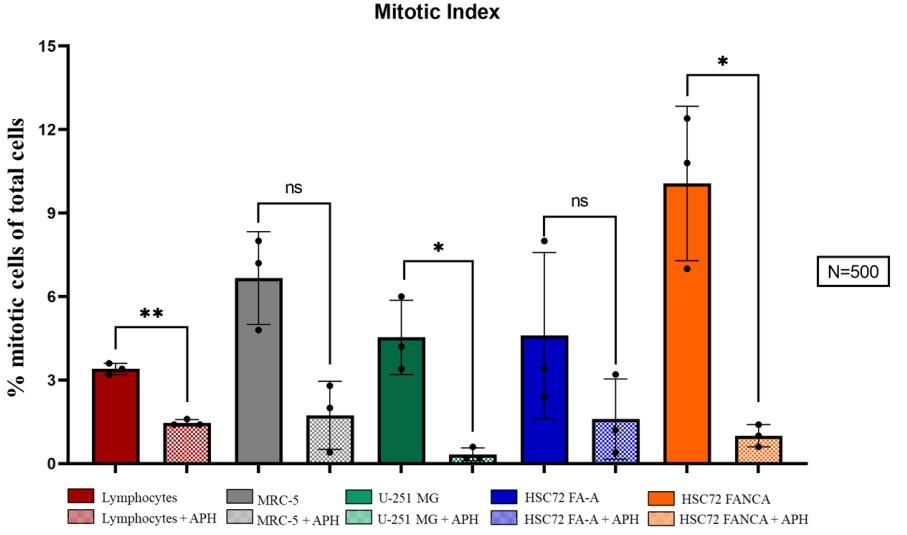

Figure 3. Percentage of M.I. (Mitotic Index) in lymphocytes (red), MRC-5 fibroblasts (grey), U-251 MG GBM cells (green), HSC72 FA-A (blue) and HSC72 FANCA (orange) in control and APH-treated conditions. The color coding of the cell types is maintained throughout the figures. The error bars represent the standard deviation (SD) of 3 independent experiments (N=500 cells for each replicate). Paired t test was used to calculate the p values, where $p>0.05$ ns, *$p\leq0.05$, **$p<0.01$, ***$p<0.001$.

I then assessed the frequency of nuclear blebbing, nucleoplasmic bridges and micronuclei in both metaphase spreads and interphase nuclei with and without APH (Figure 4A-C).
The frequency of nuclear phenotypes provides a degree of genome damage and chromosomal instability.
Nuclear blebbing is characteristic of apoptosis/necrosis cells, nucleoplasmic bridges for unfinished cytokinesis, micronuclei for mis-segregated chromosomes.
Although not statistically significant, I observed an increase in the frequency of nuclear blebbing upon APH treatment in both FA lymphoblasts cell lines (Figure 4A, graph). Similarly, I observed a trend of increased nucleoplasmic bridges in 4 out of 5 APH-treated cell lines (Figure 4B, graph). Micronuclei formation decreased in the GBM and the corrected HSC72 FANCA cell lines upon APH treatment (Figure 4C, graph).
These results suggest that APH-treated cells are likely arrested before entry into mitosis or after chromosomal segregation in G1; conclusively, low-dose APH triggers very mild phenotypes.

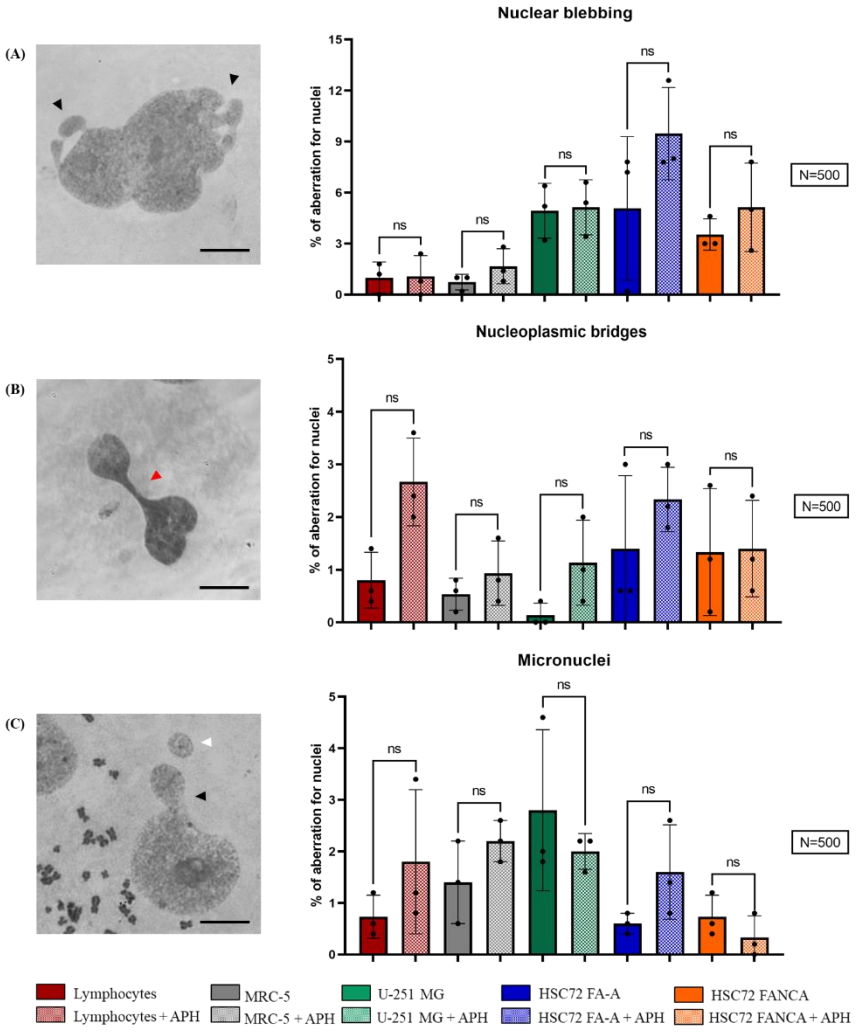

Figure 4. Percentage of nuclear aberrations: nuclear blebbing (A, black arrows), nucleoplasmic bridges (B, red arrow) and micronuclei (C, white arrow). Scale bar: 10 µm. The error bars represent standard deviation (SD) of 3 independent experiments (N=500 nuclei for each replicate). Paired t test for p values $p>0.05$ ns (not significant), $*p\leq0.05$, $**p<0.01$, $***p<0.001$.

The effect of APH treatment in mitotic cells was also evaluated on mitotic chromosomes that displayed good morphology and R-banding. This analysis implies the investigation of hundreds of metaphases of which only ~100 are considered for characterization, as described in

the Genetic Toxicology and Chromosome Aberrations guidelines by the OECD (OECD, 2016).
Changes in morphology and chromosome structure could be indicators of genetic damage (Clare, 2012).
I analyzed 100 metaphases where chromosome aberrations such as bi/tri-radials, double minutes (DMs), fragments, extra-chromatin, fragile chromatin and dicentric chromosomes were scored (Figure 5A).
As expected, several of these phenotypes were present in untreated GBM cells and in HSC72 FA-A lymphoblasts, while they were completely absent in lymphocytes derived from healthy individuals. The APH treatment affected the total number of chromosome aberrations in GBM and in both FA lymphoblasts lines but not in lymphocytes (Figure 5B, graphs).
More specifically, the frequency of DMs, DNA fragments and extra chromatin - but not of radials and fragile chromatin - decreased upon APH treatment in GBM cells. Similarly, a slight decrease of radials and extra chromatin was also observed in the corrected HSC72 FANCA cells, suggesting potential activation of checkpoints or repair upon replication stress in U-251 MG and in the corrected HSC72 FANCA cells.

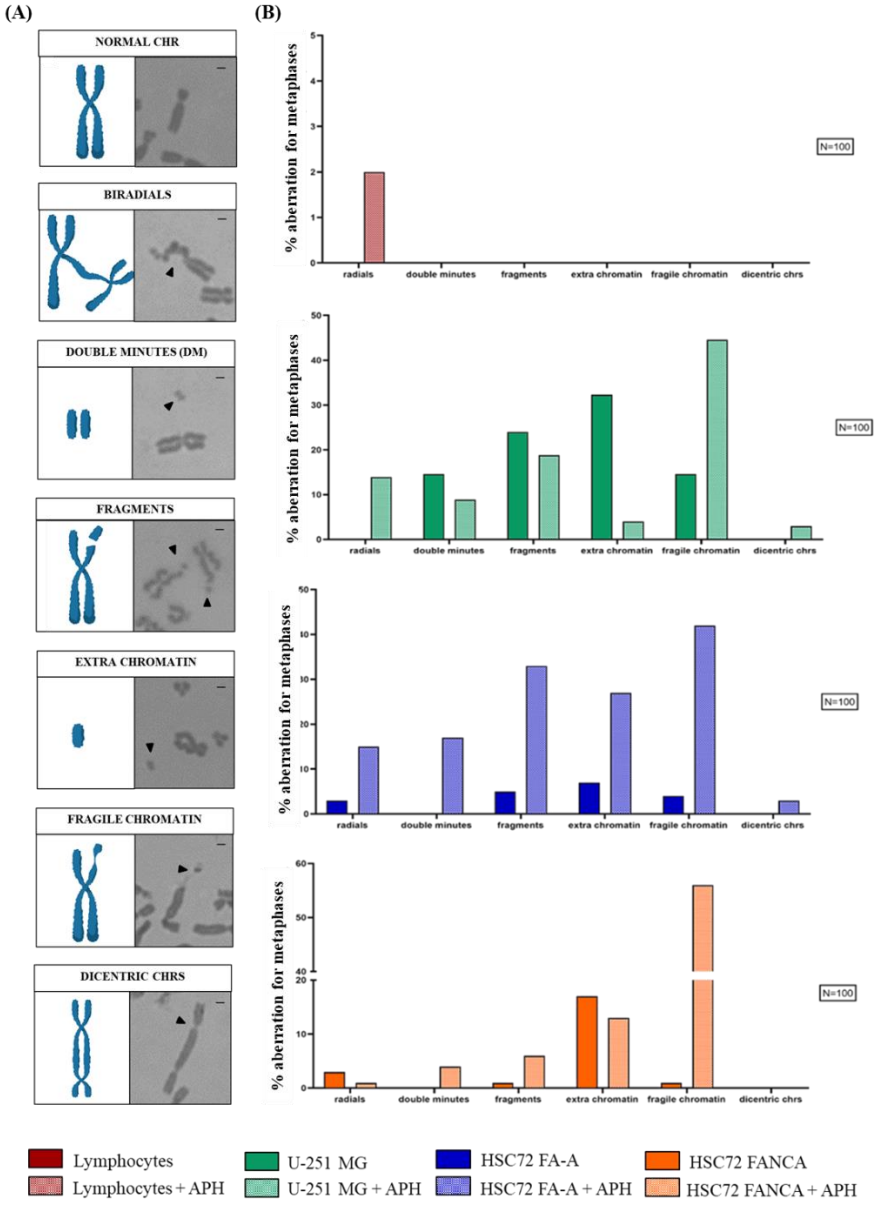

Figure 5. Representation of chromosome aberrations (A). A cartoon model (left panel) and Giemsa staining (right panel) can be seen for each scored aberration: normal chromosome, radials, double minutes (DM), fragments, extra chromatin, fragile chromatin, dicentric chromosomes. In the graphs (B), the average number of chromosome aberrations was counted per metaphases. Number of counted metaphases was 100 for each control and APH-treated conditions (N=100). Scale bar: 1 µm.

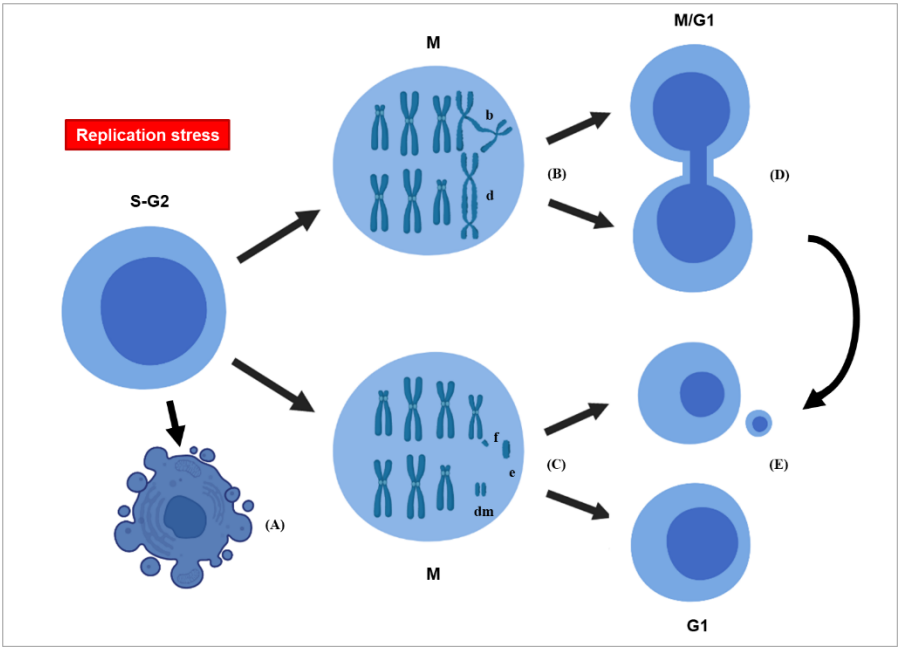

Figure 6. Model of chromosomal structural aberrations (s-CIN) and nuclear aberrations (n-CIN). The effects of replication stress in S/G2-phase could lead to structural chromosome defects (B)(C) and then chromosome mis-segregation. Errors in chromosome segregation can result in nuclear blebbing that is a feature of apoptotic/necrotic cell (A), nucleoplasmic bridges (D) and micronuclei (E). Chromosomal aberrations: b, radials; d, dicentric chromosome; f, fragments; e. extra chromatin; dm, double minutes.

The data on chromosome aberrations recapitulated the observations made for the nuclear phenotypes. Every nuclear phenotype reflects the structural chromosome aberrations found in these cells.

Replication stress can lead to apoptotic/necrotic cells (nuclear blebbing) and to a chromosomes mis-segregation that results in un uncompleted cytokinesis (nucleoplasmic bridges) or chromosome loss (micronuclei) (Figure 6).

It has been shown that chromosome segregation errors promote structural chromosome aberrations (Janssen et al., 2011; Siri et al., 2021). A proper chromosome segregation is established during the DNA synthesis, thus S-phase needs to be carefully regulated (Funk et al., 2016).

The pericentromeric heterochromatin on long arm of chromosomes 1, 9 and 16 presents as a morphological variant in a sub-condensed state named "qh+" and visible as a secondary constriction was also analyzed on 100 metaphase spreads (Figure 7A-C).
In the human karyotype, only chromosome 1, 9, 16 and the distal part of the long arm of Y exhibit this structural peculiarity (Sipek Jr et al., 2014). Under-condensed pericentromeric chromatin in both GBM cells and FA lymphoblasts was highly increased upon APH treatment, except for 16qh+ in HSC72 FA-A, while no change in qh+ expression was observed between untreated and APH-treated lymphocytes. The "qh+" variant on chromosome 16 was also observed before treatment in lymphocytes and in both HSC72 FA cell lines (Figure 7D, graphs).
Next, the incidence of DNA gaps/breaks under normal and replication stress conditions and their occurrence within CFSs was investigated. The same metaphases were stained with Giemsa and CRMA3 (Chromomycin A3) to detect both expression of the site and the specific cytogenetic band involved in the gap/break (Figure 8A). Notably, gaps and breaks were mainly identified after APH treatment within FSs in all cell types, except for the HSC72 FA-A lymphoblasts where these chromosome aberrations were already detected (Figure 8B, graphs).
Altogether, the data show that all cell types are highly affected by agents of replication stress even at a low-dose of APH, leading to a decrease in overall number of mitoses and specific fragile chromosome phenotypes.
This implies chromatin fragility in GBM cells and FA lymphoblasts.

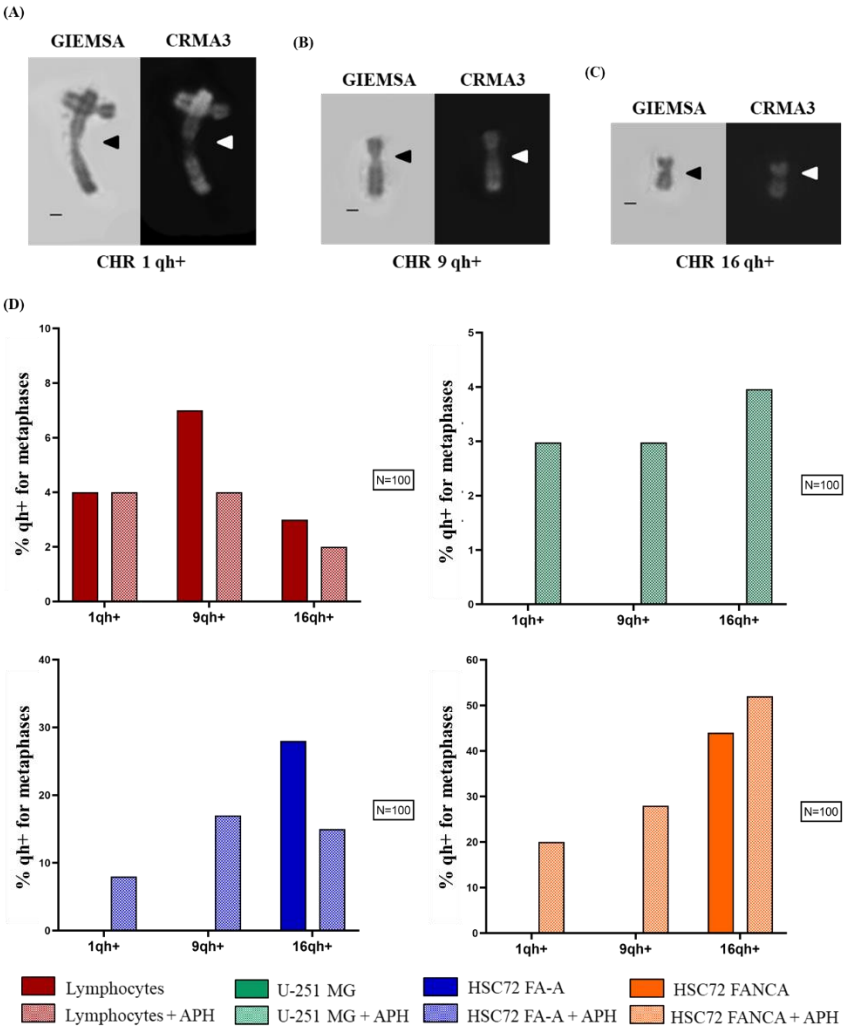

Figure 7. Sub-condensed pericentromeric regions (qh+) on chromosome 1 (A), 9 (B) and 16 (C). Percentage of each qh+ on chromosome 1, 9 and 16 in lymphocytes, glioblastoma cells and in both FA lymphoblasts lines in control and low APH conditions (D). Black arrows indicate qh+ in Giemsa staining and white arrow the qh+ in CRMA3 staining. Number of counted metaphases in control and APH-treated conditions was 100 (N=100). CHR: chromosome. Scale bar: 1 µm.

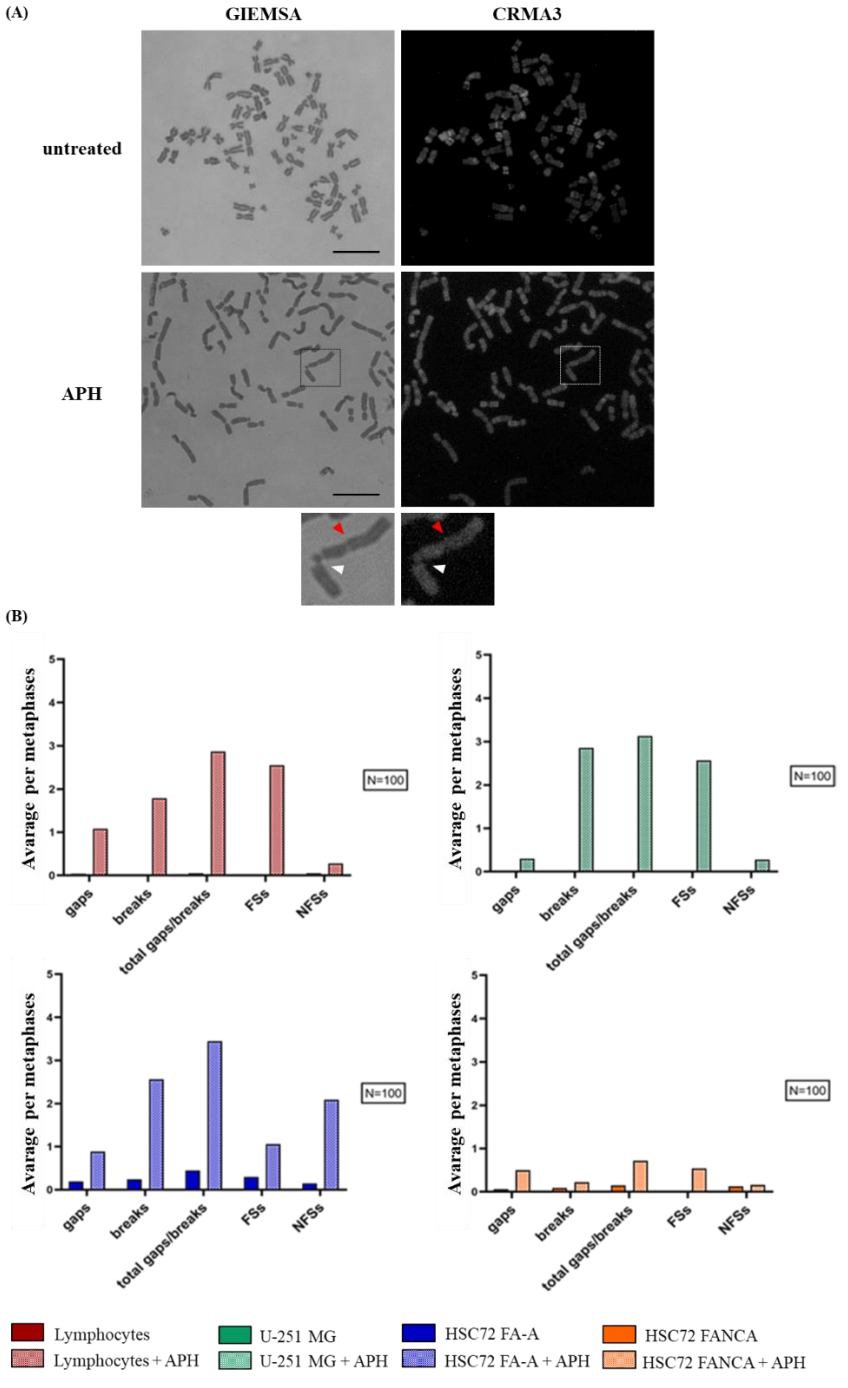
(A)
GIEMSA
CRMA3
untreated
APH
(B)
Avarage per metaphases
N=100
gaps
breaks
total gaps/breaks
FSs
NFSs
Lymphocytes
Lymphocytes + APH
U-251 MG
U-251 MG + APH
HSC72 FA-A
HSC72 FA-A + APH
HSC72 FANCA
HSC72 FANCA + APH

Figure 8. Example of cytological observation in Giemsa and CRMA3 staining. U-251 MG metaphase stained with Giemsa and CRMA3 in control and APH-treated conditions; the brackets highlight chromosome 2, where white arrows indicate the break within FRA2E (2p12-13) and red arrows the gap within FRA2F (2q22) (A). The graphs show the average number of gaps/breaks per metaphases in every cell type in control and treated conditions, and how many of these lesions were Fragile Sites (FSs) or Non-Fragile Sites (NFSs) (B). Number of counted metaphases in control and APH-treated conditions was 100 (N=100). Scale bar: 10 μm.

Replication stress induces Glioblastoma-specific CFSs expression

Cytogenetic observation of over 100 metaphases enabled to detect and mapping of the gaps/breaks to CFSs on glioblastoma metaphase chromosomes. All known human CFSs across primary cells (lymphocytes and MRC-5 fibroblasts) and GBM cells were then scored. In GBM cells, 52 CFSs were found expressed as gaps/breaks; among them, only 17 CFSs showed fragility with a frequency equal to at least 1% on the total of gaps/breaks upon APH treatment (Figure 9G, graph). Importantly, two of these CFSs localized to regions FRA2E (2p13-p12) and FRA2F (2q22) appeared to be glioblastoma-specific since the gaps/breaks induced by APH were only seen in U-251 MG cells (Figure 9B) and were not found in lymphocytes or fibroblasts under these experimental conditions. In line with previous evidence, data show the striking heterogeneity in expressing specific CFSs at different frequencies across the three cell types. For all cells, the FSs did not occur without replicative stress. After APH is supplemented to the cell culture medium, high expression of specific FSs such as FRA2E (2p13-p12) and FRA2F (2q22) (Figure 9G, graph) were found in the GBM cell line. The effect of APH in promoting CFSs expression varies in frequency between lymphocytes and U-251 MG cells. For instance, FRA3B site (3p14) (Figure 9C) in lymphocytes has an expression greater than 19%, while in GBM cells it is less than 3% (Figure 7G, graph). Conversely, glioblastoma-specific breaks localized to regions FRA2E (2p13-p12) and FRA2F (2q22) were only seen in U-251 MG cells but not observed in either lymphocytes or fibroblasts. FRA16D (16q23.2) (Figure 9F) appears as a CFS in all three cell types, potentially underscoring a different mechanism of fragility of this region that is not tissue-specific.

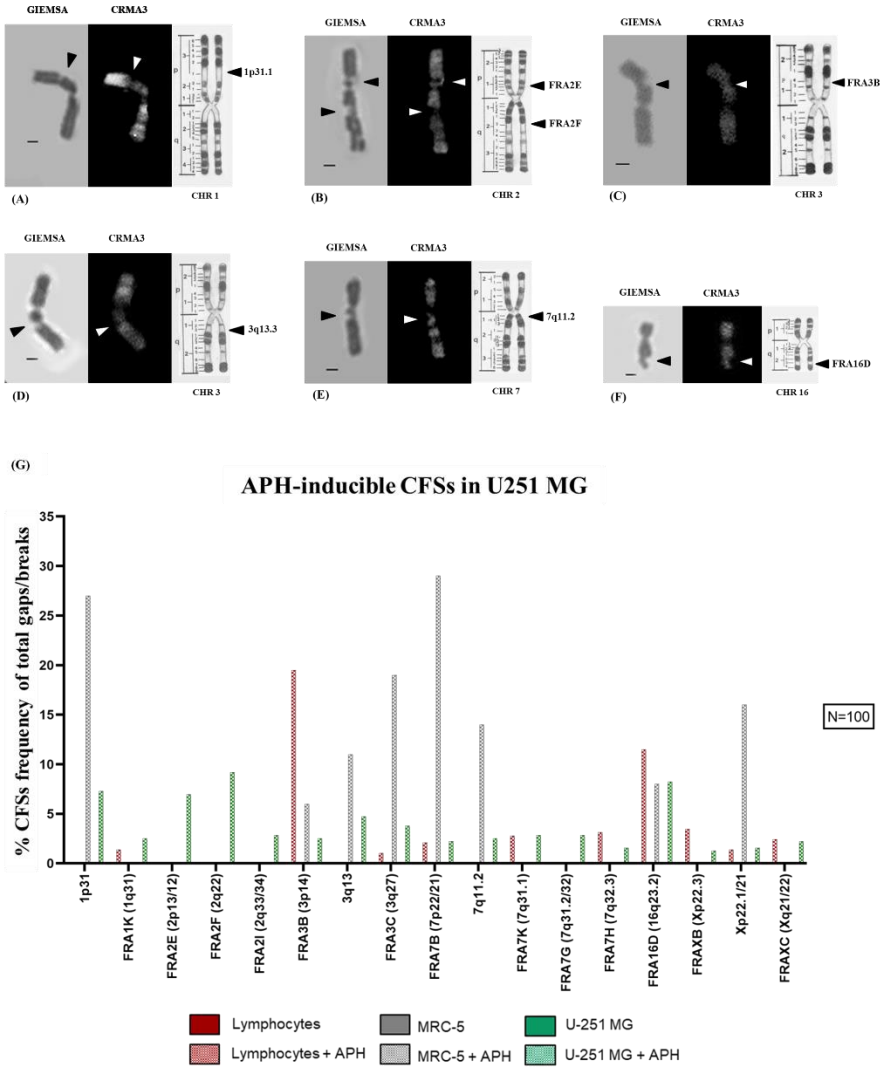

Figure 9. Representation of the most expressed CFSs in U-251 MG cells under stressful condition: 1p31.1 (A), FRA2E (2p13-12) and FRA2F (2q22) (B), FRA3B (3p14) (C), 3q13.3 (D), 7q11.2 (E), FRA16D (16q23.2) (F). R-banding by CRMA3 staining allows the recognition of the cytological band where the lesion is localized (chromosome ideograms are modified from Dutrillaux et al., 1976). In the graph (G), CFSs expressed under APH treatment with an expression frequency equal to at least 1% of the total number of gaps/breaks in lymphocytes, fibroblasts and glioblastoma cells. Number of counted metaphases for control and APH-treated conditions was 100 (N=100). CHR: chromosome. Scale bar: 1 µm.

Moreover, several characteristic fibroblast sites were identified, such as 1p31.1 (Figure 9A), 3q13.3 (Figure 9D) and 7q11.2 (Figure 9E), as previously shown (Murano et al., 1989; Le Tallec et al., 2011; Maccaroni et al., 2020), that were also expressed as gaps and breaks in GBM (Figure 7G, graph).
CFSs exhibited a very distinctive expression frequency in different cell types underscoring the tissue-specificity expression of CFSs (Le Tallec et al., 2011; Maccaroni et al, 2020) and pointing to potential glioblastoma-specific vulnerability upon replication stress within CFSs FRA2E (2p13-p12) and FRA2F (2q22) seen in U-251 MG cells.
Given the specificity of the CFSs FRA2E (2p13-p12) and FRA2F (2q22) expression in GBM, the sequence composition and the presence of transcripts within these regions was analyzed. A detailed characterization was obtained by using different databases (NCBI, Ensembl, GeneCards).
Interestingly, several long transcriptionally active genes in the brain tissue were found together with many antisense and intronic RNA transcripts that may also contribute to promote glioblastoma-specific chromosomal fragility (Figure 10A-B).

(A)

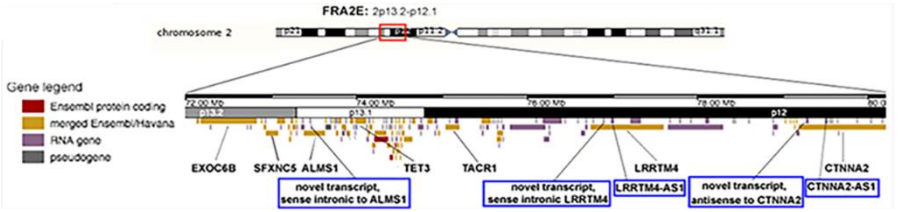

GENE NAME	DESCRIPTION	FUNCTION
EXOC6B, exocyst complex component 6B	Location: 72,175,984- 72,826,041 reverse strand Length: 650,050 nt RPKM 8.7 ± 0.34	Component of the exocyst complex involved in the docking of exocytic vesicles with fusion sites on the plasma membrane.
SFXN5, sideroflexin 5	Location: 72,175,984- 72,826,041 reverse strand Length: 129,677 nt RPKM 13.0 ± 4.6	Mitochondrial amino-acid transporter
ALMS1, centrosome and basal body associated protein	Location: 73,385,758- 73,609,919 forward strand Length: 224,162 nt RPKM 1.39 ± 0.34	Required for proper formation and/or maintenance of primary cilia (PC), microtubule-based structures that protrude from the surface of epithelial cells
TET3, tet methylcytosine dioxygenase 3	Location: 73,982,036- 74,135,394 forward strand Length: 153,359 nt RPKM 2.94	Dioxygenase that converts of 5mC into 5hmC and plays a key role in epigenetic chromatin reprogramming in the zygote following fertilization
TACR1, tachykinin receptor 1	Location: 75,046,463- 75,199,520 reverse strand Length: 153,058 nt RPKM 1.38 ± 0.97	Receptor for the tachykinin neuropeptide. It is probably associated with G proteins that activate a phosphatidylinositol-calcium second messenger system
LRRTM4, leucine rich repeat transmembrane neuronal 4	Location: 76,747,685- 77,593,319 reverse strand Length: 774,692 nt RPKM 5.6 ± 1.098	Involved in development and maintenance of the vertebrate nervous system
CTNNA2, catenin alpha 2	Location: 79,505,054- 80,648,788 forward strand Length: 1,143,735 nt RPKM 26.7 ± 12.117	Regulates morphological plasticity of synapses and cerebellar and hippocampal lamination during development

(B)

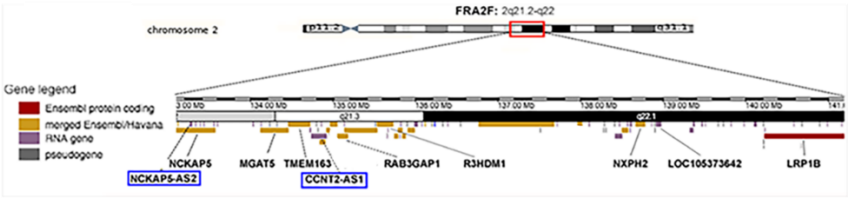

GENE NAME	DESCRIPTION	FUNCTION
NCKAP5, NCK associated protein 5	Location: 132,671,788- 133,675,182 reverse strand Length: 1,003,395 nt RPKM 0.6 ± 0.14	Involved in microtubule bundle formation and microtubule depolymerization
MGAT5, MGAT5 alpha-1,6-mannosylglycoprotein 6-beta-N-acetylglucosaminyltransferase	Location: 134,119,922- 134,454,621 forward strand Length: 334,700 nt RPKM 11.216 ± 1.51	Catalyzes the addition of beta-1,6-N-acetylglucosamine to the alpha-linked mannose of biantennary N-linked oligosaccharides present on the newly synthesized glycoproteins
TMEM163, transmembrane protein 163	Location: 134,455,759- 134,719,000 forward strand Length: 265,176 nt RPKM 3.11 ± 0.553	Predicted to enable zinc ion binding activity
RAB3GAP1, RAB3 GTPase activating protein catalytic subunit 1	Location: 135,052,292- 135,176,394 forward strand Length: 124,387 nt RPKM 16.8 ± 3.52	Catalytic subunit of a GTPase activating protein that has specificity for Rab3 subfamily. May participate in neurodevelopmental processes
R3HDM1, R3H domain containing 1	Location: 135,531,455- 135,725,270 forward strand Length: 193,786 nt RPKM 20.1 ± 6.77	No data available. Diseases associated with R3HDM1 include Ichthyosis, Congenital, Autosomal Recessive 11 and Autosomal Recessive Congenital Ichthyosis
NXPH2, neurexophilin 2	Location: 138,669,157- 138,780,390 reverse strand Length: 111,234 nt RPKM 2,1 ± 0.867	Signaling molecules that resemble neuropeptides and act by binding to alpha-neurexins and possibly other receptors
LOC105373643	Location: 139,234,673- 139,379,146 reverse strand Length: 144,474 nt RPKM 1.8 ± 2.466	Uncharacterized ncRNA
LRP1B, LDL receptor related protein 1B	Location 140,231,423- 142,132,463 reverse strand Length: 1,901,041 nt RPKM 3.0 ± 1.531	Potential cell surface proteins that bind and internalize ligands in the process of receptor-mediated endocytosis

Figure 10. Schematic representation of the unique and most expressed fragile sites in U-251 MG glioblastoma cells: FRA2E (2p13.2-p12.1) (A) and FRA2F (2q21.2-q22) (B). In every ideogram, only the genes that are primarily expressed in the brain are indicated. Colors correspond to different genes localized in these specific regions (delimited by the red brackets). Highlighted genes in blue brackets are the antisense RNAs (asRNAs) and intronic RNAs (itRNAs). Three Human Genome Resources were used to identify the gene composition and description (NCBI Genome Data Viewer, Ensembl, GeneCards).

Replication stress induces Fanconi Anemia-specific CFSs expression

Cytogenetic CFSs mapping on Fanconi lymphoblastoid cell lines (HSC72 FA-A and HSC72 FANCA) was performed on 100 metaphase spreads.

Unsurprisingly, untreated FA cells (HSC72 FA-A) revealed the assumed CFSs fragility (Figure 11G, graph) showing FRA1K (1q31), FRA2G (2q31) (Figure 11A), FRA2H (2q32) (Figure 11B), FRA6H (6p21) (Figure 11D) and FRA16D (16q23.2) (Figure 11F).

In lymphocytes and in corrected HSC72 FANCA lymphoblasts, CFSs were observed only under APH stress condition and with a similar CFSs pattern, except for FRA1F (1q31) and FRA6H (6p21) which were exclusively expressed in HSC72 FANCA cells (Figure 11H).

In total, 16 CFSs were observed in HSC72 FA-A and 19 CFSs in HSC72 FANCA with a frequency equal to at least 1% on the total of gaps/breaks (Figure 11G-H, graphs).

Among them, FRA3B (Figure 11C), FRA3C and FRA7B (Figure 11E) were expressed in all cell types, revealing a non-peculiar basis of fragility.

CFSs that were specifically expressed more than 1% in HSC72 FA-A were FRA6H (6p21), FRA13A (13q13.3) and FRA14C (14q24), while FRA1F (1q21) and FRA6H (6p21) in HSC72 FANCA (Figure 11G-H, graphs).

Cytological analysis highlighted the underlying fragility of a sensitive background such as Fanconi Anemia mutated cells (HSC72 FA-A), revealing also an interesting CFSs expression pattern.

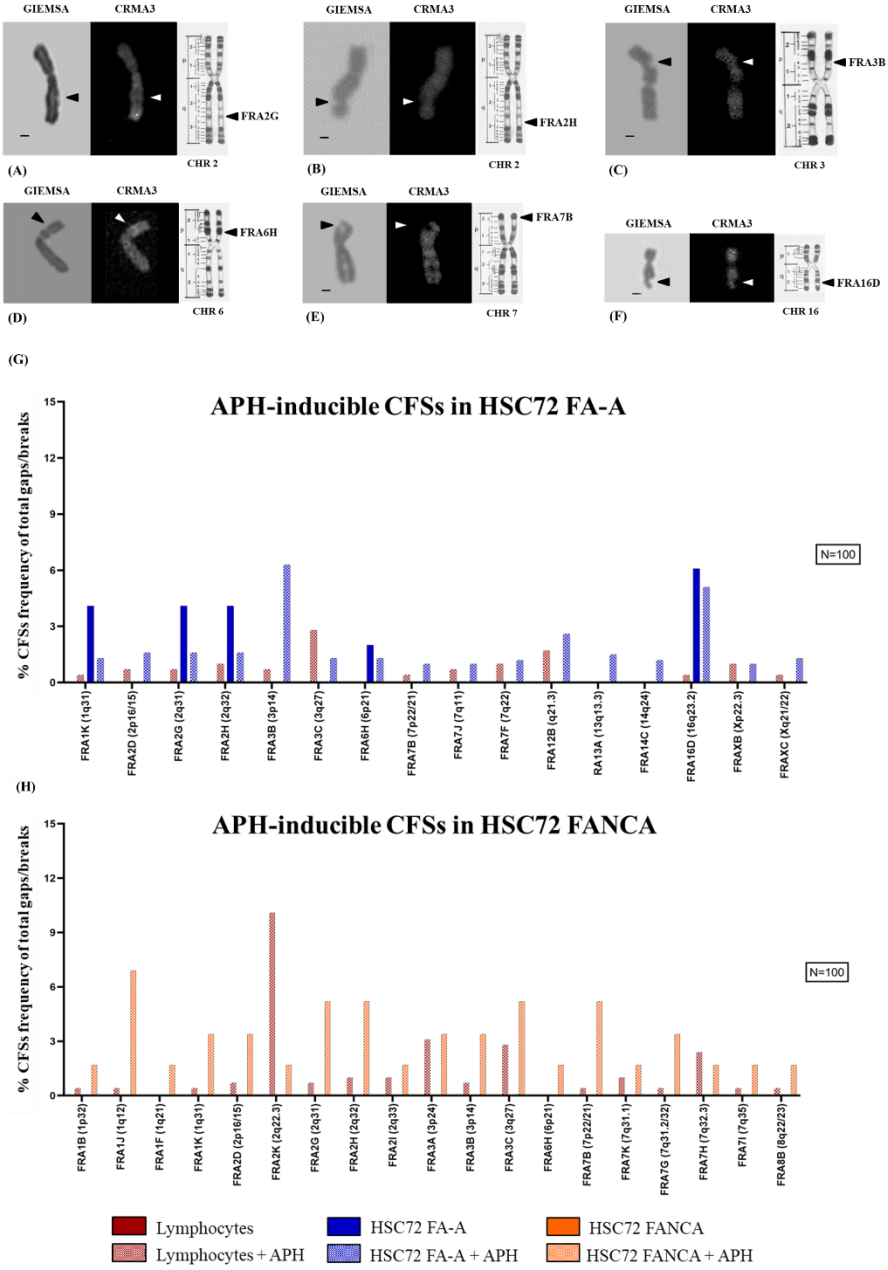

Figure 11. Representation of the most expressed CFSs in HSC72 lymphoblasts under stressful condition: FRA2G (2q31) (A), FRA2H (2q32) (B), FRA3B (3p14) (C), FRA6H (6p21) (D) and FRA7B (7p22/21) (E), FRA16D (16q23.2) (F). R-banding by CRMA3 staining allows

the recognition of the cytological band where the lesion is localized (chromosome ideograms are modified from Dutrillaux et al., 1976). In the graphs, CFSs expressed under APH treatment with an expression frequency equal to at least 1% of the total number of gaps/breaks in lymphocytes, HSC72 FA-A (G) and HSC72 FANCA (H). Number of counted metaphases for control and APH-treated conditions was 100 (N=100). CHR: chromosome. Scale bar: 1 μm.

Molecular analysis of FRA6H region was performed, as FRA6H is specifically expressed in both FA lymphoblasts lines.
NCBI, Ensembl, GeneCards databases were used to characterize long active genes in white blood cells. Remarkably in 6p21.1-p22 region there are many genes involved in the development of immunological competence for the cells of the immune system (Figure 12).

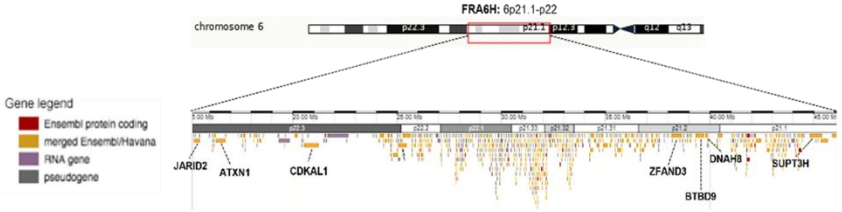

GENE NAME	DESCRIPTION	FUNCTION
JARID2, Jumonji AT Rich Interactive Domain 2	Location: 15,246,527-15,522,252 forward strand Length: 275,726 nt RPKM 3,974 ±1,047	DNA-binding protein that functions as a transcriptional repressor. This protein interacts with the Polycomb repressive complex 2 (PRC2) which plays an essential role in regulating gene expression during embryonic development
ATNX1, Ataxin 1	Location: 6,299,343-16,761,722 reverse strand Length: 462,380 nt RPKM 1,779 ± 0,389	Chromatin-binding factor that repress Notch signaling in the absence of Notch intracellular domain by acting as a CBF1 corepressor
CDKAL1, CDK5 Regulatory Subunit Associated Protein 1 Like 1	Location: 20,534,688-21,232,63 forward strand Length: 697,948 nt RPKM 1,23 ± 0,276	Member of the methylthiotransferase family. The function of this gene is not known.
ZFAND3, Zinc Finger AN1-Type Containing 3	Location: 37,787,275-38,122,400 forward strand Length: 335,126 nt RPKM 9.29 ± 0.642	Zinc finger protein involved in nucleic acid recognition, transcriptional activation, protein folding and assembly
BTBD9, BTB Domain Containing 9	Location: 38,136,227-38,607,924 reverse strand Length: 471,698 nt RPKM 1.163 ± 0.228	BTB/POZ domain-containing protein involved in protein-protein interactions
DNAH8, Dynein Axonemal Heavy Chain 8	Location: 38,683,117-38,998,301 forward strand Length: 315,185 nt RPKM 0.234 ± 0.168	Heavy chain of an axonemal dynein
SUPT3H, Suppressor Of Ty 3 Homolog	Location: 44,777,054-45,345,690 reverse strand Length: 568,637 nt RPKM 0.384 ± 0,117	Part of SAGA complex and transcription factor TFTC complex. Involved in histone H3 acetylation and histone deubiquitination.

Figure 12. Schematic representation of the unique and most express fragile sites in both HSC72 FA lymphoblastoid lines: FRA6H (6p21.1-p22). In the ideogram, only the genes that are primarily expressed in the white blood cells are indicated. Colors correspond to different genes localized in this specific region (delimited by the red bracket). Three Human Genome Resources were used to identify the gene composition and description (NCBI Genome Data Viewer, Ensembl, GeneCards).

Replication Timing of APH-inducible CFSs

Replication stress can affect the dynamics of replication during S-phase within fragile regions. To analyze the CFSs replication timing, a specific FISH probe was used for each fragile region. The FISH spots indicate the replication status of the CFS: one spot for the non-replicated allele (Figure 13, yellow arrows) and double spots for the replicated alleles (Figure 13, white arrows). Immunofluorescence (IF) against BrdU on the same nuclei revealed each specific sub-stages of S-phase from the pattern of replication foci (early, mid, late; Figure 13). The combined FISH-IF can monitor the CFS behavior throughout S-phase. These replication data were also compared with the replication analysis in lymphocytes. More than 100 nuclei for each FISH probe were observed both in the absence and the presence of APH.

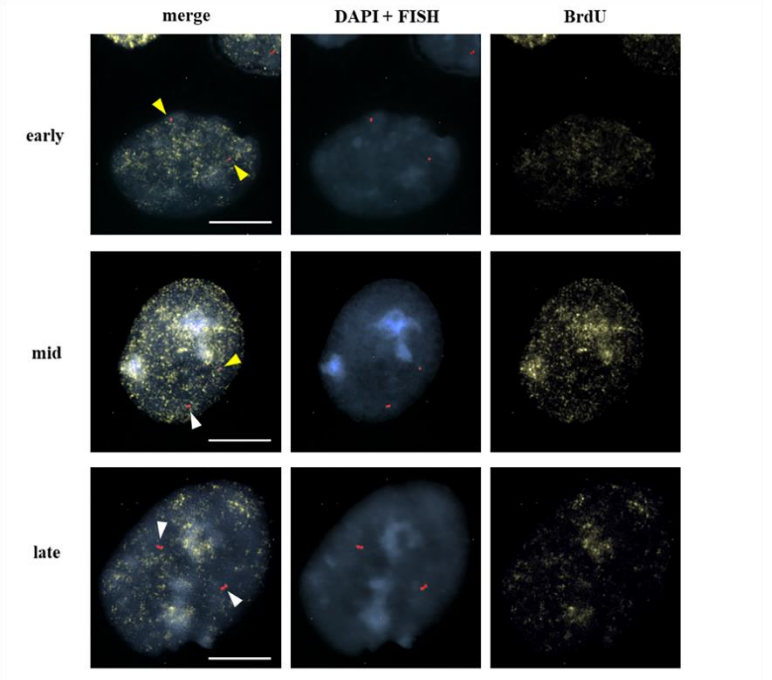

Figure 13. Example of nuclei stained with DAPI (blue), FISH spots for 3q13.3 with probe RP11-324H4 (red), and BrdU (yellow) as indicated, and merge (left) of early, mid, and late S-phase stages (D). Non-replicated alleles are single spots (yellow arrows), while replicated alleles are double spots (white arrows). Scale bar: 10 µm.

CFSs Replication Timing in U-251 MG cells

Comparing the replication timing of three CFSs expressed in U-251 MG cells (1p31.1, 3q13.3, 7q11.2) and previously studied in MRC-5 fibroblasts (Maccaroni et al., 2020) and lymphocytes, it was possible to understand the replication trend of each fragile sites in different tissues, and especially in normal and cancer cells.

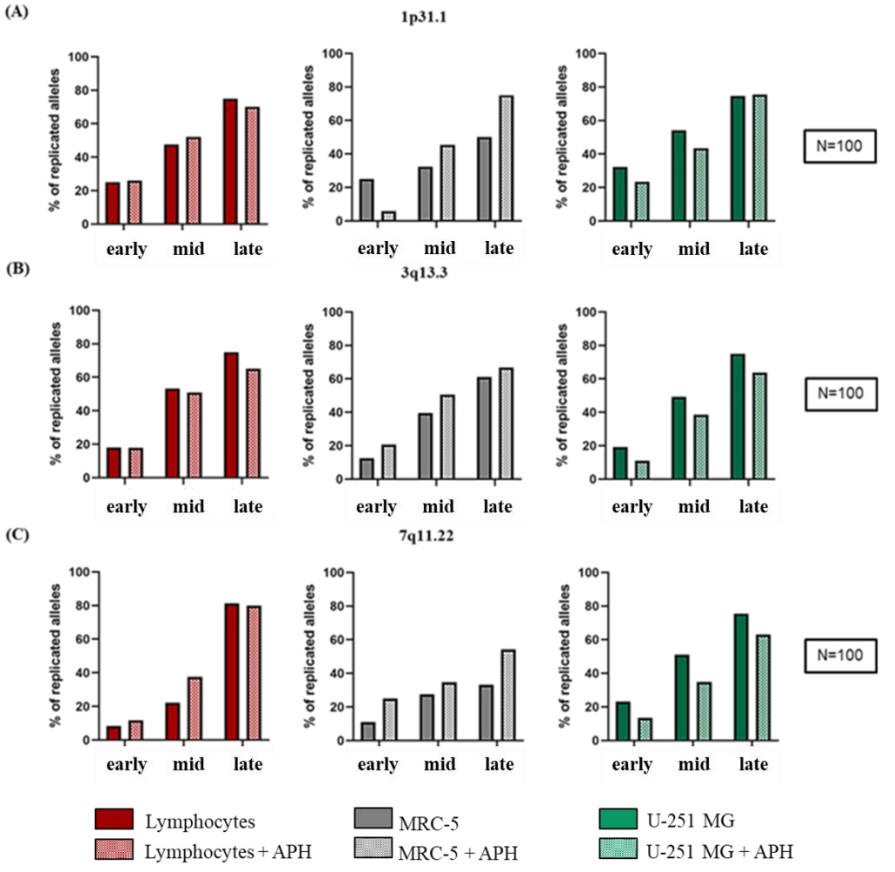

Figure 14. Replication timing of three CFSs in lymphocytes (red), MRC-5 fibroblasts (grey) and U-251 MG GBM cells (green). The graphs represent the replicated alleles in each sub-stages of S-phase for 1p31.1 (A), 3q13.3 (B), 7q11.2 (C). Number of counted nuclei for control and APH-treated conditions was 100 (N=100).

In the untreated control cells, the site 1p31.1 showed only 50% of replicated alleles in MRC-5 fibroblasts in late S-phase; under APH

treatment an increase of the total amount of replicated alleles (until ~ 75%) was observed in late S-phase, as seen in APH-treated U-251 MG cells and lymphocytes (Figure 14A).
For 3q13.3, it was not observed any difference between untreated and treated cells in spite of being a highly expressed CFS in GBM (Figure 9G, graph). In U-251 MG cells and lymphocytes under APH stress, there was a ~ 5% reduction of replicated alleles compared to control in late S-phase (Figure 14B).
Regarding the Fragile Site 7q11.2, in lymphocytes it reached the same percentages of replicated alleles in late S-phase in both normal and replicative stress conditions. Under APH, U-251 MG cells showed a slight decrease of replicated alleles, while MRC-5 fibroblasts showed a ~ 10% increase of replicated alleles in late S-phase (Figure 14C).
However, for all the analyzed samples, incomplete replication for these alleles was assessed, highlighting a possible delay in replication after late S-phase/G2-phase.
Collectively, these results show no considerable difference in replication dynamics within these regions whether they were non-fragile (lymphocytes) or expressed as CFSs at different frequencies (U-251 MG and MRC-5 fibroblasts) (Table 1).

Lymphocytes	MRC-5	U-251 MG
1p31 in normal condition		
Replicated alleles: 75% Expression frequency: 0%	Replicated alleles: 50% Expression frequency: 0%	Replicated alleles: 75% Expression frequency: 0%
1p31 in APH condition		
Replicated alleles: 70% Expression frequency: 0%	Replicated alleles: 75% Expression frequency: 27%	Replicated alleles: 76% Expression frequency: 7,3%
3q13 in normal condition		
Replicated alleles: 75% Expression frequency: 0%	Replicated alleles: 61% Expression frequency: 0%	Replicated alleles: 75% Expression frequency: 0%
3q13 in APH condition		
Replicated alleles: 65% Expression frequency: 0%	Replicated alleles: 67% Expression frequency: 11%	Replicated alleles: 64% Expression frequency: 4,8%
7q11 in normal condition		
Replicated alleles: 81% Expression frequency: 0%	Replicated alleles: 33% Expression frequency 0%	Replicated alleles: 76% Expression frequency 0%
7q11 in APH condition		
Replicated alleles: 80% Expression frequency: 0%	Replicated alleles: 54% Expression frequency: 14%	Replicated alleles: 63% Expression frequency: 2,53%

Table 1. Summary of the replication timing and expression of the three CFSs (1p31, 3q13, 7q11) in lymphocytes, MRC-5 fibroblasts and U-251 MG glioblastoma cells.

CFSs Replication Timing in HSC72 FA lymphoblasts

The replication timing of the two CFSs FRA2H and FRA7B were studied in normal lymphocytes and in both FA lymphoblasts lines, pathological and corrected background.

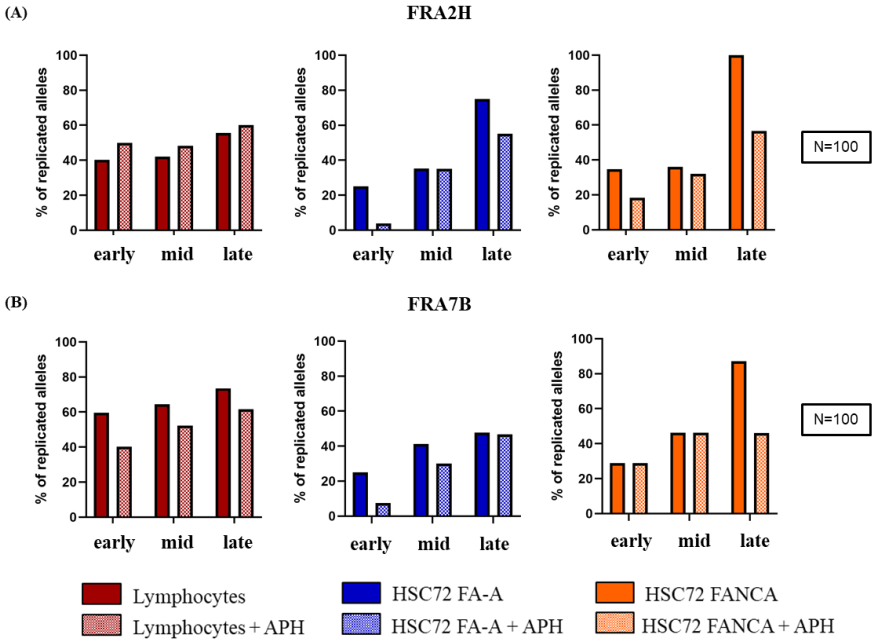

Figure 15. Replication timing of two CFSs in lymphocytes (red), HSC72 FA-A (blue) and HSC72 FANCA (orange). The graphs represent the replicated alleles in each sub-stages of S-phase for FRA2H (2q32) (A) and FRA7B (7p22) (B). Number of counted nuclei for control and APH-treated conditions was 100 (N=100).

FRA2H begins replicating early in lymphocytes reaching merely the ~ 60% of replicated alleles in late S-phase in both control and treated condition. In lymphocytes, FRA2H is not expressed as gap/break without a mild replicative stress, since the remaining non replicated alleles could replicate in G2-phase or even in mitosis.
In untreated mutated HSC72 FA-A lymphoblasts, FRA2H expression is strictly correlated with its partial replication (~ 75% of replicated alleles).

In corrected HSC72 FANCA lymphoblasts, FRA2H arrives with 100% of replicated alleles at the end of S-phase, in fact it did not show fragility. In both FA lymphoblasts cell lines upon APH condition, FRA2H shows a similar faulty trend (Figure 15A).
The analysis of the replication timing of FRA7B in lymphocytes under normal and stressful conditions indicates only a partial replication of alleles. For the mutated HSC72 FA-A, FRA7B replication timing is impaired in both control and treated conditions, suggesting an intrinsic fragility of this site in FA background.
In corrected HSC72 FANCA, the replication behavior of FRA7B follows a linear trend, indicating a normal replication timing, while in stressful condition replication timing appears quite regular, despite the replication slows down in late S-phase with 54% of non-replicated alleles (Figure 15B).
Replication timing analysis revealed how the compromised repair pathway of FA is essential to guarantee the completion of the replication process, especially in stressful conditions where all cells slow down (Table 2).

Lymphocytes	HSC72 FA-A	HSC72 FANCA
FRA2H in normal condition		
Replicated alleles: 56% Expression frequency: 0%	Replicated alleles: 75% Expression frequency: 4,1%	Replicated alleles: 100% Expression frequency: 0%
FRA2H in APH condition		
Replicated alleles: 60% Expression frequency: 1%	Replicated alleles: 55% Expression frequency: 1,6%	Replicated alleles: 57% Expression frequency: 5,2%
FRA7B in normal condition		
Replicated alleles: 74% Expression frequency: 0%	Replicated alleles: 48% Expression frequency: 0%	Replicated alleles: 87% Expression frequency: 0%
FRA7B in APH condition		
Replicated alleles: 62% Expression frequency: 0%	Replicated alleles: 47% Expression frequency: 1%	Replicated alleles: 46% Expression frequency: 5,2%

Table 2. Summary of the replication timing and expression frequency of two CFSs (FRA2H and FRA7B) in lymphocytes and in the two isogenic FA lymphoblasts lines.

Cytological effects under DAPI treatment in Fanconi Anemia cells

Above, I discussed the fragile sites induced by the APH treatment, an exogenous stress that deals with S-phase and prolongs until mitosis. In this paragraph, I report the cytological observations on nuclei and mitotic chromosomes after DAPI treatment for 18 hrs (DAPI 50 µg/ml for lymphocytes and DAPI 5 µg/ml for both FA cell lines) in lymphocytes and in the two isogenic FA lymphoblast lines.
DAPI is known to be a fluorescent nucleic acid stain but it can also act as a DNA under-condensing agent in G2-phase (Prantera et al., 1981). Fanconi Anemia cells have a prolonged G2-phase upon DNA damage because of the lack of efficient FA repair pathway and the chromatin sub-condensation produced by DAPI could allow the fragile sites to be available and thus receptive to other pathways.
Before the characterization of DAPI inducible CFSs, cytological observations for both nuclei and metaphase phenotypes were carried out. These results (Figure 16 and Figure 17) show no particular cytotoxic effect of DAPI emerges, although it caused a slight reduction in the proliferation rate in all cell lines (Figure 16) and increased cell blebbing in the two isogenic FA lymphoblasts cell lines (Figure 17A, graph).

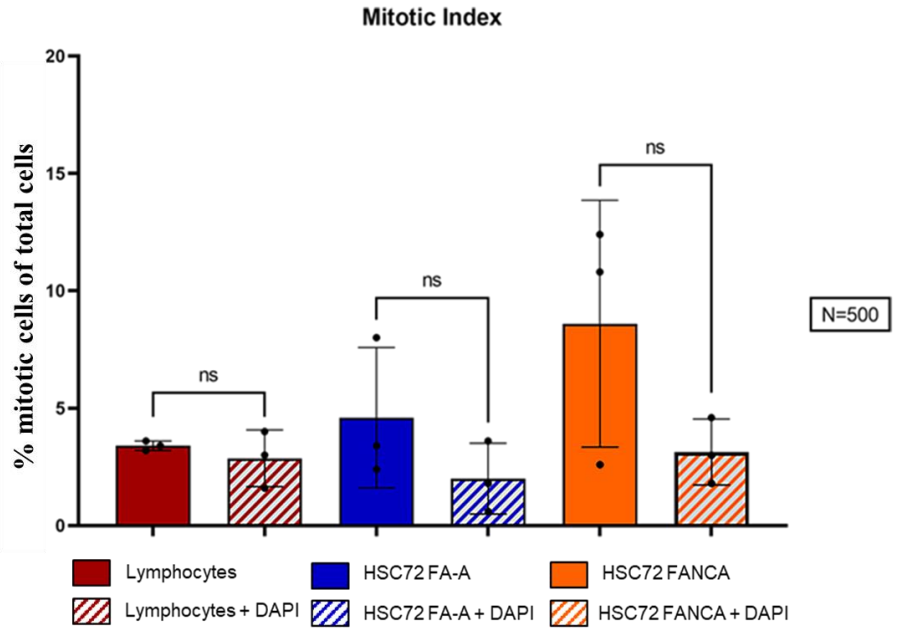

Figure 16. Percentage of M.I. (Mitotic Index) in lymphocytes (red), HSC72 FA-A (blue) and HSC72 FANCA (orange) in control and DAPI-treated conditions. The error bars represent the standard deviation (SD) of 3 independent experiments (N=500 cells for each replicate). Paired t test was used to calculate the p values, where $p>0.05$ ns, $*p\leq0.05$, $**p<0.01$, $***p<0.001$.

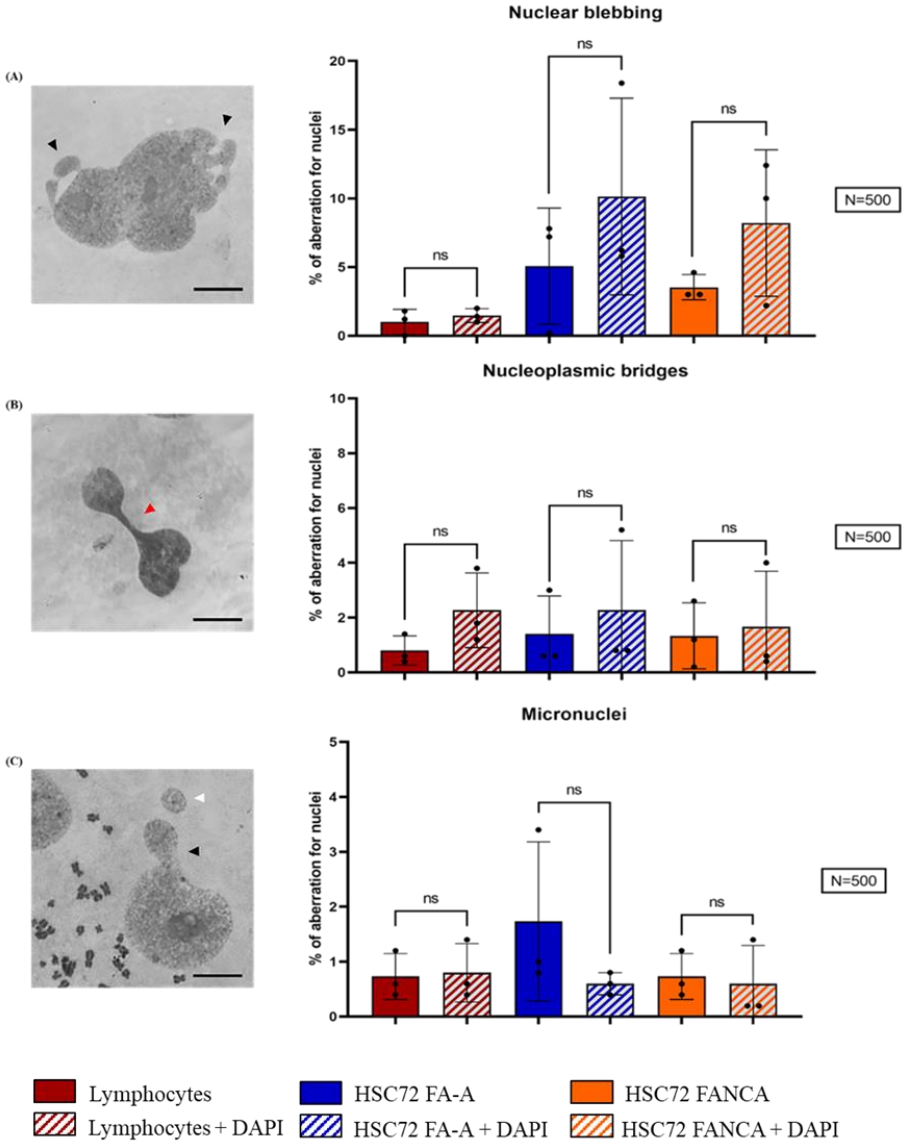

Figure 17. Percentage of nuclear aberrations: nuclear blebbing (A, black arrows), nucleoplasmic bridges (B, red arrow) and micronuclei (C, white arrow). Scale bar: 10 µm. The error bars represent standard deviation (SD) of 3 independent experiments (N=500 nuclei for each replicate). Paired t test for p values $p>0.05$ ns (not significant), $*p\leq0.05$, $**p<0.01$, $***p<0.001$.

Upon DAPI treatment, a greater amount of DNA fragments and fragile chromatin have been noted in lymphocytes and corrected HSC72 FANCA cells (Figure 18B, graphs), showing a fragility of sub-telomeric and telomeric regions (AT-rich sequences) in the presence of this compound. In mutated HSC72 FA-A cells, DAPI contributed to double minutes, extra chromatin and dicentric chromosomes formation (Figure 18B, graphs).
A similar effect upon DAPI addition can be seen on the pericentromeric heterochromatin on the long arm of chromosomes 1, 9 and 16 in lymphocytes, and not in the two lymphoblasts cell lines where the mild increase of qh+ variant implied chromosomes 1 and 9 (Figure 19D, graphs).
In lymphocytes and in corrected HSC72 FANCA cells treated with DAPI, a total increase in gaps/breaks was observed, unlike the mutated HSC72 FA-A cells (Figure 20B, graphs).
Furthermore, it is interesting to note that the proportion of gaps to total gaps/breaks increased after DAPI addition in all three cell types, indicating an evident lack of condensation due to the addition of DAPI in the culture medium.
These data suggest that DAPI could make the chromatin more accessible to DDR pathways, leading to decondensed chromosome regions.
Gaps/breaks quantification under DAPI treatment appears to concord with the FSs observation.

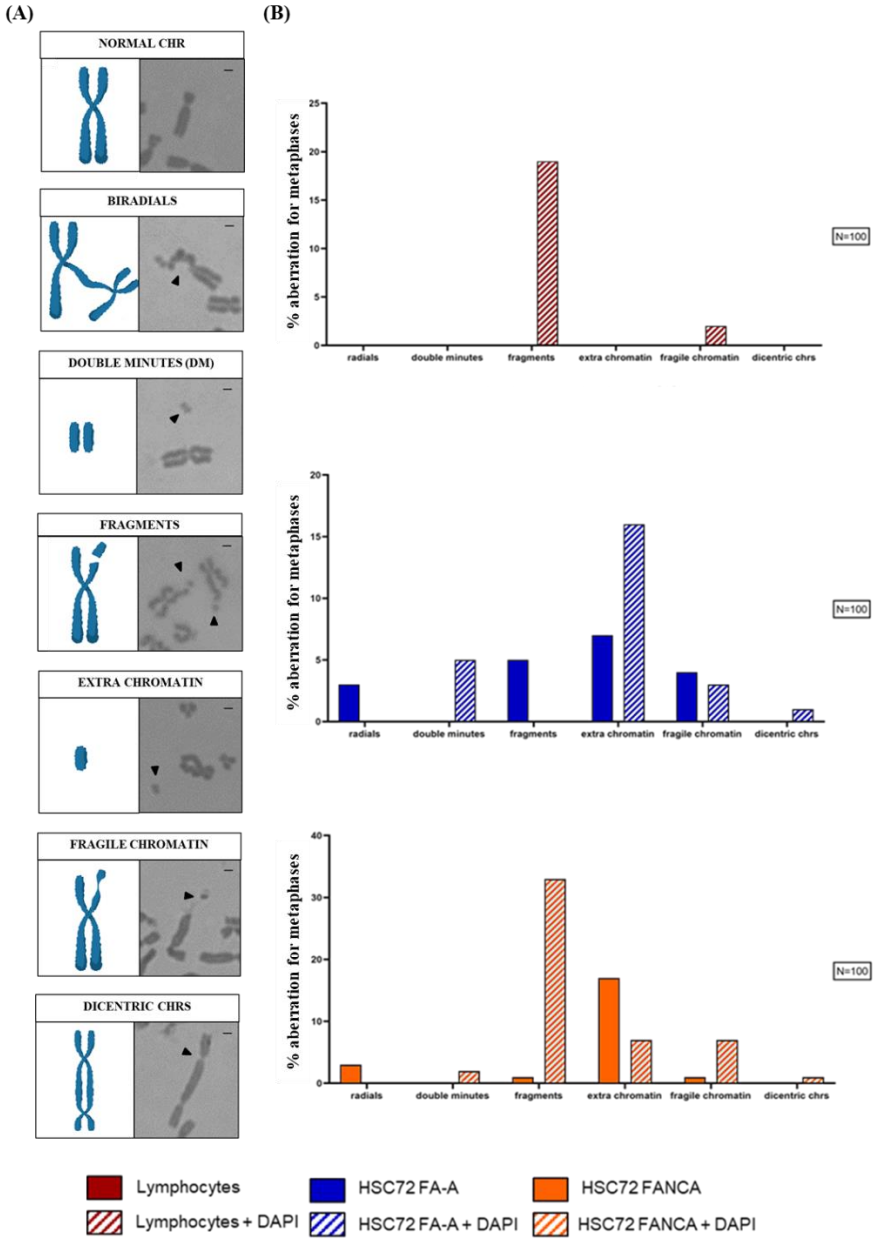

Figure 18. Representation of chromosome aberrations (A). A cartoon model (left panel) and Giemsa staining (right panel) can be seen for each scored aberration: normal chromosome, radials, double minutes (DM), fragments, extra chromatin, fragile chromatin, dicentric chromosomes. In the graphs (B), the average number of chromosome aberrations was counted

per metaphase. Number of counted metaphases was 100 for each control and DAPI-treated conditions (N=100). Scale bar: 1 µm.

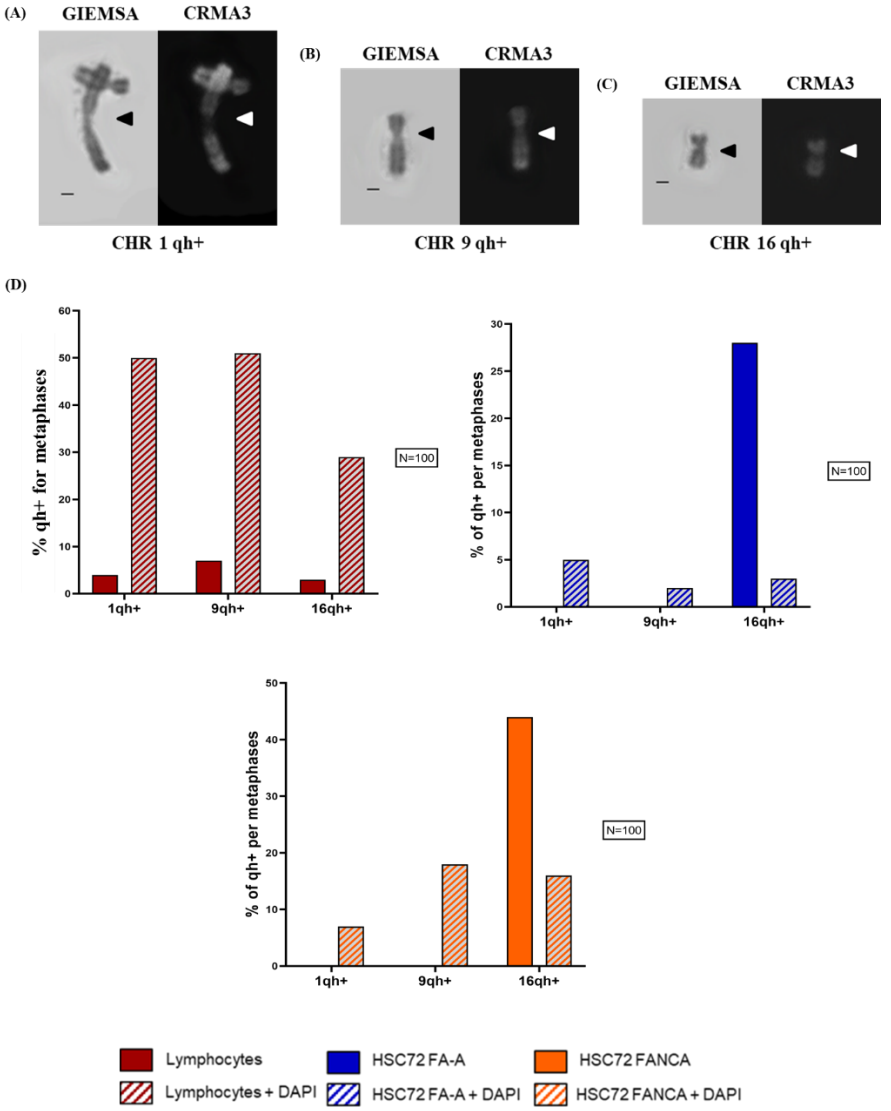

Figure 19. Sub-condensed pericentromeric regions (qh+) on chromosome 1 (A), 9 (B) and 16 (C). Percentage of each qh+ on chromosome 1, 9 and 16 in lymphocytes and in both FA lymphoblasts lines in control and DAPI conditions (D). Black arrows indicate qh+ in Giemsa staining and white arrow the qh+ in CRMA3 staining. Number of counted metaphases in control and DAPI-treated conditions was 100 (N=100). CHR: chromosome. Scale bar: 1 µm.

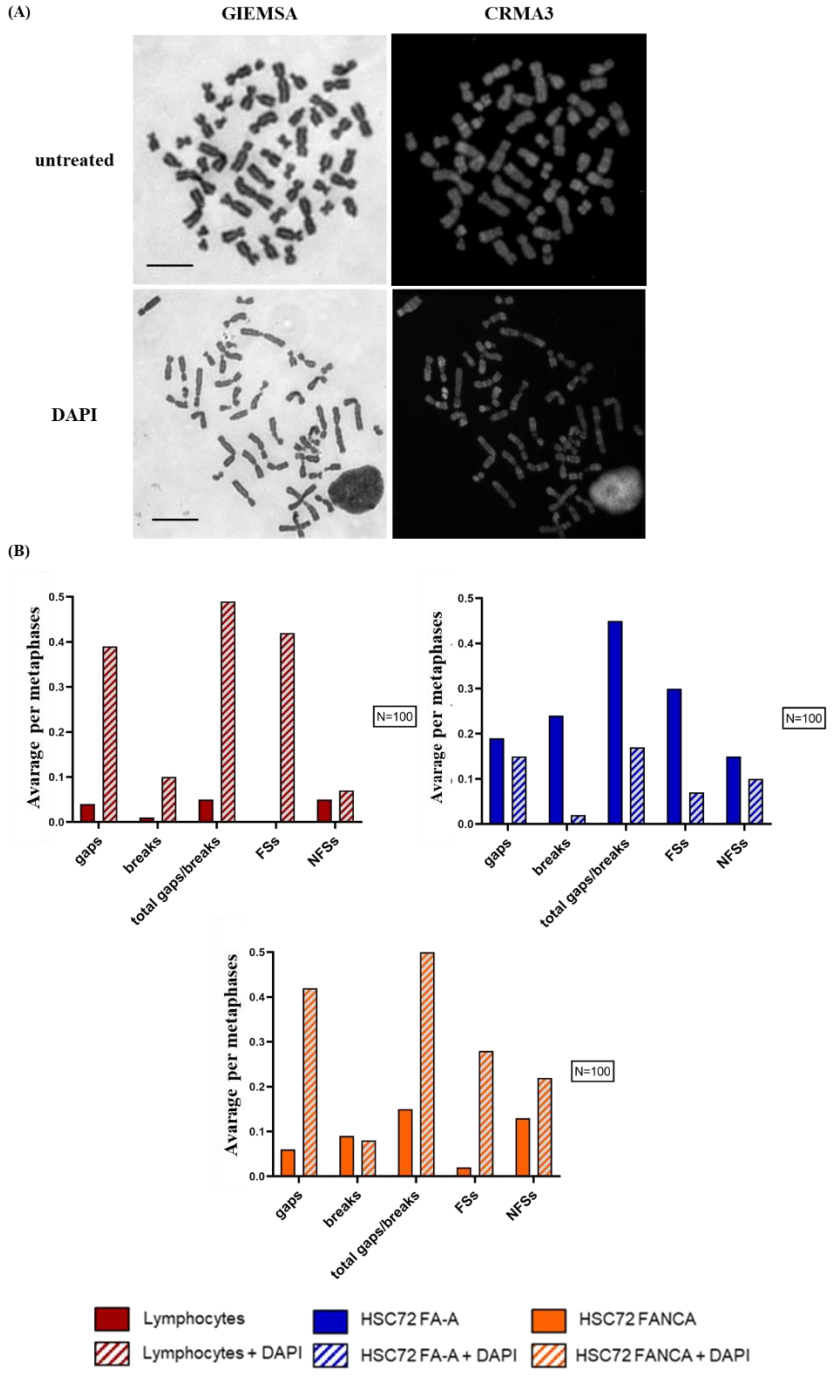
(A)
GIEMSA
CRMA3
untreated
DAPI
(B)
Avarage per metaphases
N=100
gaps
breaks
total gaps/breaks
FSs
NFSs
Lymphocytes
Lymphocytes + DAPI
HSC72 FA-A
HSC72 FA-A + DAPI
HSC72 FANCA
HSC72 FANCA + DAPI

Figure 20. Example of cytological observation in Giemsa and CRMA3 staining. HSC72 FA-A metaphase stained with Giemsa and CRMA3 in control and DAPI-treated conditions (A). The graphs show the average number of gaps/breaks per metaphase in every cell type in control and treated conditions, and how many of these lesions were Fragile Sites (FSs) or Non-Fragile Sites (NFSs) (B). Number of counted metaphases in control and DAPI-treated conditions was 100 (N=100). Scale bar: 10 µm.

DAPI-inducible CFSs

It is worth noticing the different expression pattern of CFSs induced by DAPI in the two lines of FA lymphoblasts (Figure 21D-E, graphs). After treatment with DAPI, CFS that occurred in control condition in Fanconi anemia cells (HSC72 FA-A) were no longer expressed, apart from FRA2G (2q31) (Figure 21D, graph) which is recognized to belong also to the DAPI-inducible CFSs (Pelliccia and Rocchi, 1986; Rocchi and Pelliccia, 1988; Pelliccia and Rocchi, 1992).
All CFSs induced by DAPI treatment in Fanconi Anemia cells are AT-rich regions (Limongi et al., 2003; Curatolo et al., 2008; Bosco et al., 2010).
However, CFSs exclusively expressed under DAPI treatment were present in all the three cell types (Figure 21D-E, graphs): FRA1H (1q42) (Figure 21A), FRA2G (2q31) (Figure 21B) and FRA7B (7p22) (Figure 21C).
These sites can be considered as DAPI-sensitive chromosomal regions and they seemed to have a predisposition to bind this compound and thus these regions are no longer capable of undergoing normal condensation.
Aphidicolin induced the expression of most CFSs (Figure 9 and Figure 11), whilst DAPI exposed a discrete and well defined pattern of fragile sites (Figure 21D-E, graphs).

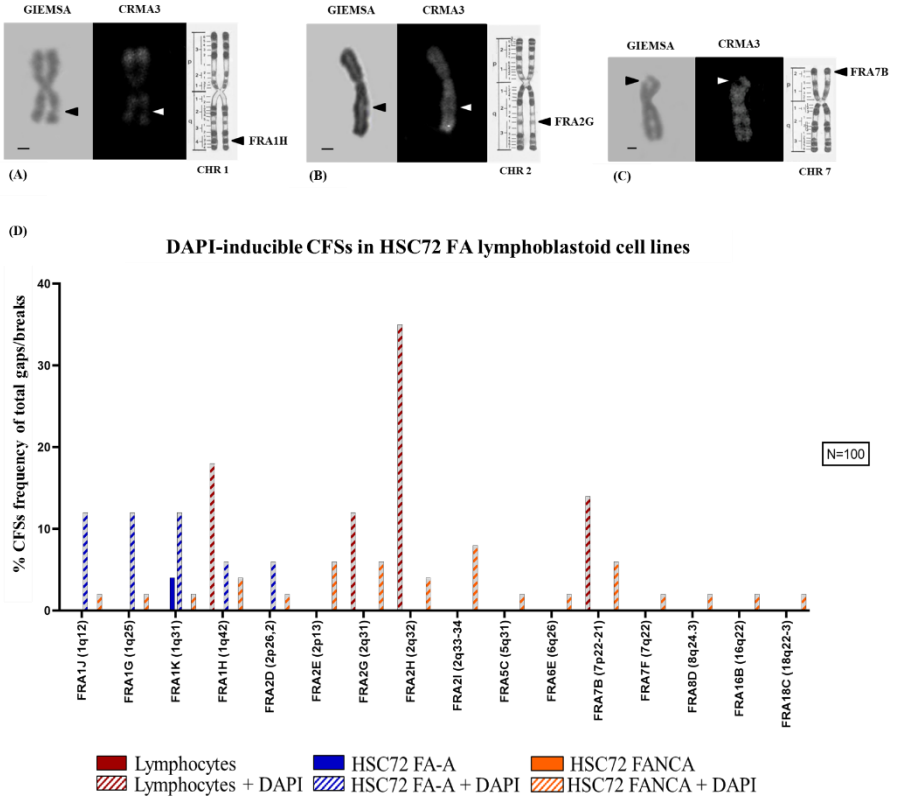

Figure 21. Representation of the most expressed CFSs in HSC72 lymphoblasts under DAPI condition: FRA1H (1q42) (A), FRA2G (2q31) (B) and FRA7B (7p22/21) (C). R-banding by CRMA3 staining allows the recognition of the cytological band where the lesion is localized (chromosome ideograms are modified from Dutrillaux et al., 1976). In the graphs, CFSs expressed under DAPI treatment with an expression frequency equal to at least 1% of the total number of gaps/breaks in lymphocytes, HSC72 FA-A (D) and HSC72 FANCA (E). Number of counted metaphases for control and DAPI-treated conditions was 100 (N=100). CHR: chromosome. Scale bar: 1 µm.

Replication Timing of DAPI-inducible CFSs

To further understand the different expression of FRA2H and FRA7B under DAPI treatment, I analyzed their replication timing during S-phase in healthy lymphocytes and in both pathological and corrected FA lymphoblasts cell lines.

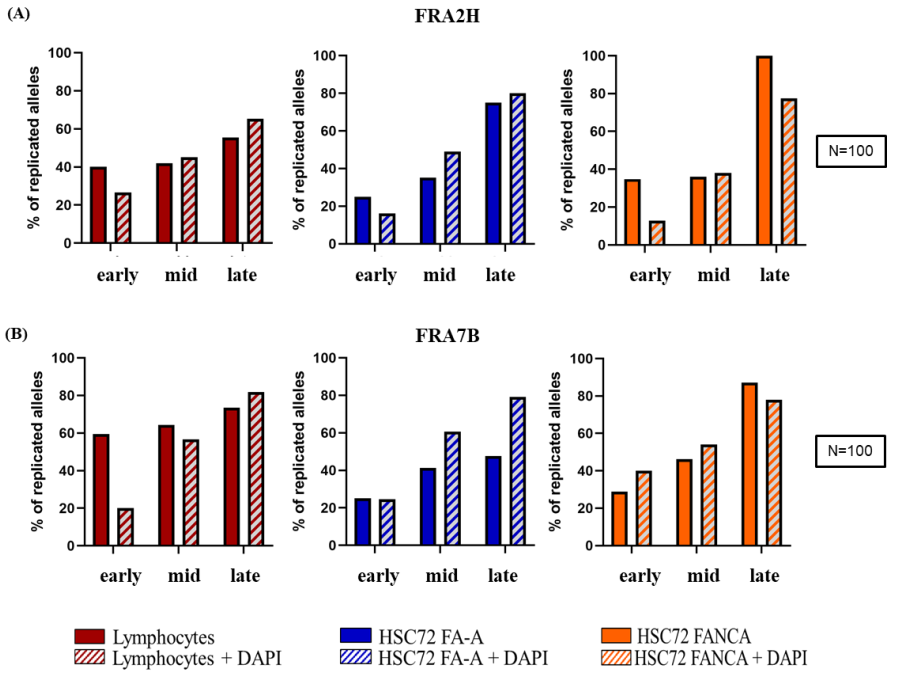

Figure 22. Replication timing of two CFSs in lymphocytes (red), HSC72 FA-A (blue) and HSC72 FANCA (orange). The graph represents the replicated alleles in each sub-stages of S-phase for FRA2H (2q32) (A) and FRA7B (7p22) (B). Number of counted nuclei for control and DAPI-treated conditions was 100 (N=100).

In lymphocytes and HSC72 FA-A lymphoblasts, the replication timing of FRA2H seemed slightly improved upon DAPI condition (around 75% of replicated alleles), even though in lymphocytes it was stated as gap/break with 35% of expression frequency; in corrected HSC72 FANCA cell line treated with DAPI, FRA2H was elicited with 4% of expression frequency, reflecting its decreasing replication trend (Figure 22A). A very mitigated beneficial effect of DAPI treatment was more pronounced for mutated FA cells than for control cells (see Table 3 for FRA2H expression frequency in both normal and treated conditions).

FRA7B exhibited analogous behavior to FRA2H, not achieving the totality of replicated alleles until late S-phase in all the three cell types (Figure 22B), where indeed it was expressed as DAPI-sensitive chromosomal regions (Table 3).

Ultimately, the combination of late replication timing and the altered DNA structure due to the presence of DAPI may leads to the onset of these peculiar CFSs.

Lymphocytes	HSC72 FA-A	HSC72 FANCA
FRA2H in normal condition		
Replicated alleles: 56% Expression frequency: 0%	Replicated alleles: 75% Expression frequency: 4,1%	Replicated alleles: 100% Expression frequency: 0%
FRA2H in DAPI condition		
Replicated alleles: 65% Expression frequency: 35%	Replicated alleles: 80% Expression frequency: 0%	Replicated alleles: 78% Expression frequency: 4%
FRA7B in normal condition		
Replicated alleles: 74% Expression frequency: 0%	Replicated alleles: 48% Expression frequency: 0%	Replicated alleles: 87% Expression frequency: 0%
FRA7B in DAPI condition		
Replicated alleles: 82% Expression frequency: 14%	Replicated alleles: 79% Expression frequency: 6%	Replicated alleles: 78% Expression frequency: 6%

Table 3. Summary of the replication timing and expression frequency of two CFSs (FRA2H and FRA7B) in lymphocytes and in the two isogenic FA lymphoblasts lines.

Replication in interphase and mitotic cells

Upon exposure to low doses of APH and DAPI treatments, all cell types suffer insults that result in chromosome instability (Figure 5 and Figure 18), including expression of specific CFSs (Figure 9, Figure 11 and Figure 21).
The analyzed CFSs in each cell type fail to duplicate within the timeframe of S-phase (Figure 14, Figure 15 and Figure 22), potentially entering mitosis unreplicated. To better understand the nature of CFSs' expression, the cell cycle distribution was evaluated using BrdU incorporation under untreated and treated conditions in U-251 MG cells and in both FA lymphoblasts lines.
The interphase nuclei were scored as either replicating (BrdU-positive nuclei, white arrows in Figure 23A) representing different stages of S-phase (as in Figure 13) or non-replicating cells (BrdU-negative, red arrows in Figure 23A).
GBM cells shift from BrdU negative to a replicative state with a significant increase in BrdU positive cells when exposed to replication stress in APH-treated cells (Figure 23B, graphs).
The higher proportion of GBM cells residing in S-phase may implies the replication struggle induced by APH and the activation of intra-S-phase checkpoint.
Differently, both FA lymphoblasts cell lines revealed an unaffected ratio of cells in S-phase under mild treatment with APH or DAPI (Figure 23B, graphs).
Unfinished replication before the onset of M-phase may cause MiDAS, a phenomenon where DNA synthesis continues into mitosis. Indeed, it was detected the presence of BrdU signals on 1 to 4 chromosomes per metaphase spread in treated conditions and on some metaphases of untreated U-251 MG cells and HSC72 FA-A lymphoblasts (Figure 23A, yellow brackets), indicating that defective replication and condensation persist into mitosis, likely contributing to the chromosome defects and resulting in gaps and breaks at specific CFS.

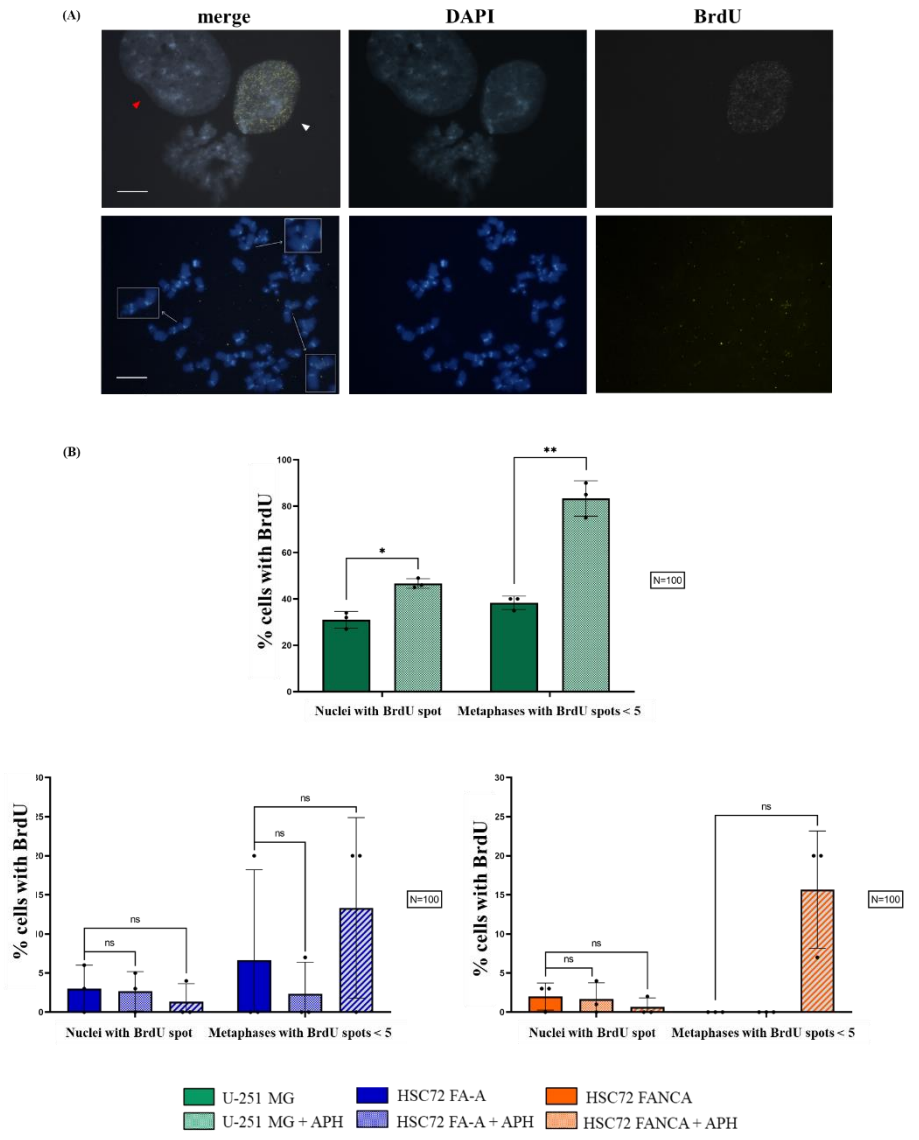

Figure 23. Metaphase spreads and interphase nuclei with BrdU foci (yellow) and DAPI staining (blue), BrdU-negative (non-replicating cells, red arrows) and BrdU-positive (replicating cells, white arrows) (A); the graphs indicate the number of BrdU-positive nuclei and metaphases with <5 BrdU spots of each cell lines in control and treated conditions (B). Scale bar: 10 μm. The error bars represent standard deviation (SD) of 3 independent experiments (N=100 nuclei for each replicate; N=15 metaphases for each replicate). Paired t test was used to calculate the p values, where $p>0.05$ ns, *$p\leq0.05$, **$p<0.01$, ***$p<0.001$.

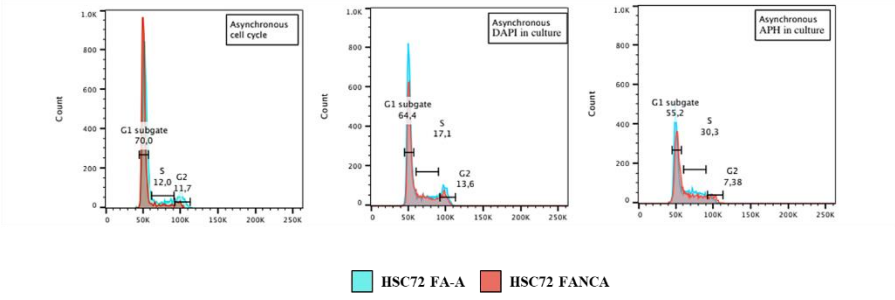

Figure 24. Flow histograms of FA lymphoblastoid cell lines in control and in APH and DAPI conditions. HSC72 FA-A in light blue and HSC72 FANCA in red.

To confirm the previous results for FA lymphoblast cell lines (Figure 23B, graphs), I analyzed the cell cycle by FACS (Fluorescence-Activated Cell Sorting).
Upon DAPI treatment, HSC72 FA-A mutant cells and HSC72 FANCA cells displayed an unvaried cell cycle but the increased S/G2-phase accumulation respect to control condition; in APH condition, the S-phase of both FA cell lines was particularly delayed and stalled (Figure 24).
Collectively, my data suggest that these chromosomal regions show cell type-specific fragility likely due to multiple converging features including the presence of long genes actively transcribed in the tissue of origin, slower/impaired replication, improper chromatin condensation and evidence of MiDAS to attempt at completing DNA synthesis at these regions ahead of chromosome segregation in mitosis.

CONCLUSIONS

My work is based on the analysis of two important aspects of CFSs expression: replication timing and post-replicative processes.
In each cell line, out of all known CFSs only those expressed after APH and DAPI treatments with a frequency equal to or greater than 1% of the total gaps/breaks were considered in this study.
Fragile sites that appear to be specific in these tissues were identified and characterized.
A comprehensive characterization of CFSs expression in U-251 MG cells and in both FA lymphoblasts cell lines under condition of mild replicative stress revealed cell type-specific CFSs.
Glioblastoma specific-CFSs induced by APH were localized to regions FRA2E (2p13-p12) and FRA2F (2q22), while in both FA lymphoblasts cell lines the CFS specificity resided in FRA6H.
In pathological conditions, DNA synthesis may be compromised by the lack of basic replication-components and DNA maintenance factors, leading to mitotic arrest (Miron et al, 2015). After APH treatment, each cell line displays a specific pattern of CFSs that is not detectable in lymphocytes. Within these APH specifically expressed CFSs, it was observed that the presence of long genes, incomplete replication and delayed DNA synthesis persisted into mitosis (MiDAS).
Data showing the replication dynamics during S-phase for U-251 MG untreated or treated cells with APH suggest that the replication issues at these sites partly activate a replication checkpoint as observed upon scoring BrdU positive and negative cells.
The different responses obtained from the two pathological cell types (Glioblastoma Multiforme and Fanconi Anemia cells) can be explained by the fact that cancer cells such as glioblastoma can bypass DNA damage and cell cycle checkpoints and proceed through the cell cycle despite the persistent damage and/or unfinished replication within the timeframe of S-phase or G2-phase. Instead, both mutated and corrected Fanconi Anemia cell lines are unable to deal with replication stress and to recover completely from the damage induced by APH. Upon DAPI, both FA lymphoblast lines proved a strong activation of mitotic DNA synthesis.

However, not all delayed/late replicating regions appear as chromosome breaks, implicating other molecular features such as an unusual chromatin conformation.
In the last part of my work, I focused on DAPI-inducible CFSs (FRA1H, FRA2G, FRA7B), to elucidate how the post-replicative phase of chromatin compaction is essential to their integrity.
Furthermore, presence of long genes, especially actively transcribed in the concerned tissues, may further enhance fragility of specific region that manifest as gaps or breaks on mitotic chromosomes.
This work offers an initial overview of Common Fragile Sites expression in glioblastoma and Fanconi Anemia that may be further exploited for future cytogenetic, molecular and clinical studies to advance our understanding of these CIN-associated diseases.

MATERIALS AND METHODS

Human cell cultures

- Peripheral blood lymphocytes: at least 5 mL of blood from an adult normal individual are cultured with sodic heparin and Phytohemagglutinin;
- HSC 72 FA-A cell line: stabilized lymphoblasts derived from a patient with Fanconi Anemia, mutated in FANCA gene. The cell line was provided by Valeria Naim Laboratory, IGR Gustave Roussy-University Paris-Saclay;
- HSC 72 FANCA cell line: stabilized lymphoblasts derived from a patient with Fanconi Anemia, carrying pG1 retroviral vector with cloned 5.5-kb FANCA cDNA (pG1-FAA5.5). The cell line was provided by Valeria Naim Laboratory, IGR Gustave Roussy-University Paris-Saclay;
- Glioblastoma Multiforme U-251 MG cell line: (Astrocytoma IV WHO grade) was purchased from "Banca Biologica and Cell Factory (Banca Biologica and Cell Factory, Genoa, Italy) and was provided by Antonio Antoccia Laboratory, Università di Roma Tre

The human glioblastoma U-251 MG cells were grown in Eagle's Minimum Essential Medium (EMEM; Euroclone) supplemented with 10% Fetal bovine serum (FBS) (Corning), 1% penicillin (Thermo Fisher Scientific) and 1% L-glutamine (Thermo Fisher Scientific) at 37 °C with 5% CO_2. Lymphocyte cultures were prepared from human peripheral whole blood of healthy individuals, collected with heparin; lymphocytes and both HSC72 FA lymphoblasts were grown in RPMI medium (Corning) supplemented with 10% FBS, 1% penicillin and 1% L-glutamine at 37 °C with 5% CO_2. For stimulation of T lymphocytes proliferation, phytohemagglutinin (PHA, GIBCO, 3%) was added to the culture medium for 72 hrs.To verify HSC 72 FA lymphoblasts cell lines, the medium was supplemented for 48 hrs with Mitomycin C (MMC) (40 nM/L). To induce Common Fragile Sites, aphidicolin (0.4 μM) was added to the cell medium for 22-24 hrs. DAPI (4′,6′-diamidino-2-phenylindole hydrochloride) was added to the medium for 18 hrs in lymphocytes (50 μg/ml) and in both

lymphoblastoid cell lines (5 µg/ml). To collect the mitotic cells, colchicine (Sigma-Aldrich) was supplemented to the medium of lymphocytes (1 mM) for 2 hrs and both HSC 72 FA lymphoblasts (1 mM) and U-251 MG cells (5 µM) for 4 hrs. For replication timing analysis, 5-Bromo-2'-deoxyuridine (BrdU; 10 µM) was added 20 min prior to harvesting the cells.

Metaphase spreads preparation

Upon colchicine treatment, lymphocytes, lymphoblasts and U-251 MG cells were harvested for metaphase spreads preparation. U-251 MG cells were trypsinized (trypsin 0.1% EDTA, Corning) and centrifuged prior to addition of hypotonic solution (KCl 0.075 M) for 20 min at 37 °C. The hypotonic treatment was performed for 8 min in lymphocytes and lymphoblasts; after centrifugation, the Ibraimov's solution (3% methanol and 5% acetic acid in dH_2O) was used only in the pelleted lymphocytes to remove the erythrocytes. Swollen cells were centrifuged twice and resuspended in cold fixative solution (methanol:acetic acid at a ratio of 3:1) and then stored overnight at -20 °C. The metaphase spreads and interphase nuclei were dropped onto clean glass slides and air-dried. The slides were stored at 4 °C until subsequent analysis.

Cytogenetic observation and analysis

The slides were stained with 4% Giemsa (Carlo Erba) to detect chromosome aberrations and then with Chromomycin A3 (R-banding) to localize gaps/breaks band locations, according to ISCN recommendation (Maccaroni et al., 2020).
Karyotype of both HSC72 FA lymphoblasts was performed by R-banding. Karyotype of this glioblastoma multiforme U-251 MG clone was performed using mFISH (multicolor-FISH) by the Antoccia Laboratory (Berardinelli et al., 2018).
The quantification of chromosome aberrations was done according to the OECD guideline (OECD, 2016).

BAC Extraction and Labelling by Nick Translation

The bacterial artificial chromosomes (BACs) were chosen from NCBI GenBank (https://www.ncbi.nlm.nih.gov/genbank/) for chromosome 1 (1p31, RP11-316C12, chr1: 71,385,313-71,476,945), chromosome 2 (2q32, RP11-315C24, chr2:184,740,00-184,920,00), chromosome 3 (3q13, RP11-324H4 chr3: 116,954,325-117,125,019) and chromosome 7 (7p21, RP4-696N1, chr7: 8,401,674 - 8,784,896; 7q11, RP11 321C7 chr7: 67,705,408 - 67,771,498).
The BAC clones were gently supplied from Dr. Mariano Rocchi, University of Bari (Italy).
Bacteria were grown in 10 mL of Luria-Bertani (LB) medium and selected with chloramphenicol (20 μg/mL). BACs were extracted by alkaline lysis and subsequently labelled by Nick Translation with bio-16-dUTP (biotin-16-deoxy-Uridine Triphosphate) and/or dig-16-dUTP (digoxigenin-16-deoxy-Uridine Triphosphate). The labeled probes were used for fluorescent *in situ* hybridization (FISH) experiments on interphase nuclei.

DNA Fluorescence *In Situ* Hybridization (FISH)

The slides were treated with RNase A (100 μg/mL in 2X Saline Sodium Citrate SSC solution) for 1 hr at 37 °C and dehydrated by washing for 5 min in 70%, 90% and 100% ethanol. After air drying, the slides were aged at 65 °C for 60 min and denatured at 80 °C for 2 min with 2X SSC 70% formamide (Sigma). The denaturation was stopped with cold 70% ethanol for 5 min, and the slides were dehydrated again with 90% and 100% ethanol and air dried prior to hybridization with the denatured probes (200 ng). The used BACs were RP11-316C12 (1p31.1), RP11-324H4 (3q13.3) and RP11 321C7 (7q11.2). Sequentially the overnight BAC probes incubation at 37 °C, 3 x 5-min post-hybridization washes with 1X SSC were performed at 60 °C. The slides were then incubated for 30 min with anti-digoxigenin-rhodamine antibody (1:20, Roche). Three washes with 2X SSC 0.1% Tween20 were performed. The slides were counterstained with DAPI (Sigma; 1 μg/mL), diluted 1:300 in Antifade VECTASHIELD Mounting Medium (Vector Laboratories).

Immunofluorescence on interphase and mitotic cells

Immunofluorescence (IF) against BrdU was performed to distinguish the different stages of the S-phase. The slides pretreated with FISH were incubated for 1 hr at room temperature with the anti-mouse BrdU monoclonal antibody (MoBU-1, Thermo Fisher Scientific), diluted 1:300 in 5% FBS in 1X PBS, pH 7.4. After 3 x 5-min washes in 1X PBS, the slides were incubated with FITC-conjugated anti-mouse IgG H&L antibody (Abcam) (1:1000 in 1X PBS, pH 7.4) for 1 hr at room temperature. After 4 x 5-min washes in 1X PBS, a DAPI:Antifade VECTASHIELD Antifade Mounting Medium (Vector Laboratories) solution (1: 300) was used to mount the slides.

Acquisition and processing of sample observations

Metaphase spreads and nuclei were observed at a 100X magnification using an epifluorescence microscope (Zeiss Axioplan) equipped with CCD camera (Charge-Coupled Device). The images of metaphase spreads and nuclei were taken using RSImage software and then processed using Photoshop (Adobe) software.

Fluorescence-Activated Cell Sorting (FACS)

For each cell line and condition, 200.000 cells were collected and centrifuged at 1000 rpm for 5 min. After the addition of 1 ml of 1X PBS 10% FBS, the cells were transfer into conical bottom tubes, centrifuged and the supernatant was discard. Then, 2 ml of 1X PBS 0.1% Sodium azide was added and centrifuged. The cells were resuspended in 300 µl of 1X PBS 50% FBS and 900 µl of 70% ethanol was added drop by drop on vortex (low speed). To stain the sample, cells were washed with 1X PBS 0.01% Sodium azide and resuspended in 150 µl of 1X PBS and 150 µl of DAPI solution (DAPI 50 µg/ml; RNAse A 40 ng/ml; 1X PBS 10% Triton X-100). The tubes were incubated for 15 min at 55 °C and then at room temperature. The samples were analyzed by Flow Cytometry Platform at CLNS IIT (BD LSRFortessa™ System).

Fragile Sites sequence analysis

In addition to fragile sites expression, we analyzed the sequence and gene composition for the region using three Human Genome Resources (NCBI Genome Data Viewer: https://www.ncbi.nlm.nih.gov/genome/gdv/ [Release Data May 16, 2021]; Ensembl: http://www.ensembl.org/Homo_sapiens/Location/Genome [Human GRCh38p13]; GeneCards: https://www.genecards.org/). The characterization is visible in Supplementary Table 1. The elements within the fragile sites characterized include location, length and gene expression.

Statistical analysis

Statistical paired t-tests were calculated on Prism (TablePad software). Individual *p* values are indicated in the Figures. P values: ns (not significant) $p>0.05$, *$p\leq0.05$, **$p<0.01$, ***$p<0.001$.

REFERENCES

1. Barcellona, M. L., & Gratton, E. (1996). Fluorescence anisotropy of DNA/DAPI complex: torsional dynamics and geometry of the complex. Biophysical Journal, 70(5), 2341–2351. https://doi.org/10.1016/S0006-3495(96)79800-4
2. Berardinelli, F., Sgura, A., Facoetti, A., Leone, S., Vischioni, B., Ciocca, M., & Antoccia, A. (2018). The G-quadruplex-stabilizing ligand RHPS enhances sensitivity of U251 MG glioblastoma cells to clinical carbon ion beams. The FEBS Journal, 285(7), 1226–1236. https://doi.org/10.1111/febs.14415
3. Berger, R., Bloomfield, C. D., & Sutherland, G. R. (1985). Report of the committee on chromosome rearrangements in neoplasia and on fragile sites. Cytogenetic and Genome Research, 40(1–4), 490–535. https://doi.org/10.1159/000132181
4. Bergoglio, V., Boyer, A.-S., Walsh, E., Naim, V., Legube, G., Lee, M. Y. W. T., Rey, L., Rosselli, F., Cazaux, C., Eckert, K. A., & Hoffmann, J.-S. (2013). DNA synthesis by Pol η promotes fragile site stability by preventing under-replicated DNA in mitosis. Journal of Cell Biology, 201(3), 395–408. https://doi.org/10.1083/jcb.201207066
5. Bhowmick, R., Minocherhomji, S., & Hickson, I. D. (2016). RAD52 Facilitates Mitotic DNA Synthesis Following Replication Stress. Molecular Cell, 64(6), 1117–1126. https://doi.org/10.1016/j.molcel.2016.10.037
6. Blin, M., le Tallec, B., Nähse, V., Schmidt, M., Brossas, C., Millot, G. A., Prioleau, M.-N., & Debatisse, M. (2019). Transcription-dependent regulation of replication dynamics modulates genome stability. Nature Structural & Molecular Biology, 26(1), 58–66. https://doi.org/10.1038/s41594-018-0170-1
7. Bosco, N., Pelliccia, F., & Rocchi, A. (2010). Characterization of FRA7B, a human common fragile site mapped at the 7p chromosome terminal region. Cancer

Genetics and Cytogenetics, 202(1), 47–52. https://doi.org/10.1016/j.cancergencyto.2010.06.008
8. Boteva, L., Nozawa, R.-S., Naughton, C., Samejima, K., Earnshaw, W. C., & Gilbert, N. (2020). Common Fragile Sites Are Characterized by Faulty Condensin Loading after Replication Stress. Cell Reports, 32(12), 108177. https://doi.org/10.1016/j.celrep.2020.108177
9. Brison, O., El-Hilali, S., Azar, D., Koundrioukoff, S., Schmidt, M., Nähse, V., Jaszczyszyn, Y., Lachages, A.-M., Dutrillaux, B., Thermes, C., Debatisse, M., & Chen, C.-L. (2019). Transcription-mediated organization of the replication initiation program across large genes sets common fragile sites genome-wide. Nature Communications, 10(1), 5693. https://doi.org/10.1038/s41467-019-13674-5
10. Buchwald, M. (1995). Complementation groups: one or more per gene? Nature Genetics, 11(3), 228–230. https://doi.org/10.1038/ng1195-228
11. Chan, K. L., Palmai-Pallag, T., Ying, S., & Hickson, I. D. (2009). Replication stress induces sister-chromatid bridging at fragile site loci in mitosis. Nature Cell Biology, 11(6), 753–760. https://doi.org/10.1038/ncb1882
12. Clare, G. (2012). The In Vitro Mammalian Chromosome Aberration Test (pp. 69–91). https://doi.org/10.1007/978-1-61779-421-6_5
13. Cortés-Ciriano, I., Lee, J. J.-K., Xi, R., Jain, D., Jung, Y. L., Yang, L., Gordenin, D., Klimczak, L. J., Zhang, C.-Z., Pellman, D. S., Akdemir, K. C., Alvarez, E. G., Baez-Ortega, A., Beroukhim, R., Boutros, P. C., Bowtell, D. D. L., Brors, B., Burns, K. H., Campbell, P. J., … Park, P. J. (2020). Comprehensive analysis of chromothripsis in 2,658 human cancers using whole-genome sequencing. Nature Genetics, 52(3), 331–341. https://doi.org/10.1038/s41588-019-0576-7
14. Debatisse, M., le Tallec, B., Letessier, A., Dutrillaux, B., & Brison, O. (2012). Common fragile sites: mechanisms of instability revisited. Trends in Genetics, 28(1), 22–32. https://doi.org/10.1016/j.tig.2011.10.003
15. Dekaban, A. (1965). Persisting clone of cells with an abnormal chromosome in a woman previously irradiated.

Journal of Nuclear Medicine : Official Publication, Society of Nuclear Medicine, 6(10), 740–746.
16. Durkin, S. G., & Glover, T. W. (2007). Chromosome Fragile Sites. Annual Review of Genetics, 41(1), 169–192. https://doi.org/10.1146/annurev.genet.41.042007.165900
17. Dutrillaux, B., Couturier, J., Richer, C.-L., & Viegas-Péquignot, E. (1976). Sequence of DNA replication in 277 R- and Q-bands of human chromosomes using a BrdU treatment. Chromosoma, 58(1), 51–61. https://doi.org/10.1007/BF00293440
18. Franchitto, A. (2013). Genome Instability at Common Fragile Sites: Searching for the Cause of Their Instability. BioMed Research International, 2013, 1–9. https://doi.org/10.1155/2013/730714
19. Funk, L. C., Zasadil, L. M., & Weaver, B. A. (2016). Living in CIN: Mitotic Infidelity and Its Consequences for Tumor Promotion and Suppression. Developmental Cell, 39(6), 638–652. https://doi.org/10.1016/j.devcel.2016.10.023
20. Glover, T. W., Arlt, M. F., Casper, A. M., & Durkin, S. G. (2005). Mechanisms of common fragile site instability. Human Molecular Genetics, 14(suppl_2), R197–R205. https://doi.org/10.1093/hmg/ddi265
21. Glover, T. W., Berger, C., Coyle, J., & Echo, B. (1984). DNA polymerase alpha inhibition by aphidicolin induces gaps and breaks at common fragile sites in human chromosomes. Human Genetics, 67(2), 136–142. https://doi.org/10.1007/BF00272988
22. Hellman, A., Zlotorynski, E., Scherer, S. W., Cheung, J., Vincent, J. B., Smith, D. I., Trakhtenbrot, L., & Kerem, B. (2002). A role for common fragile site induction in amplification of human oncogenes. Cancer Cell, 1(1), 89–97. https://doi.org/10.1016/S1535-6108(02)00017-X
23. Helmrich, A., Ballarino, M., & Tora, L. (2011). Collisions between Replication and Transcription Complexes Cause Common Fragile Site Instability at the Longest Human Genes. Molecular Cell, 44(6), 966–977. https://doi.org/10.1016/j.molcel.2011.10.013

24. Hiratani, I., Takebayashi, S., Lu, J., & Gilbert, D. M. (2009). Replication timing and transcriptional control: beyond cause and effect—part II. Current Opinion in Genetics & Development, 19(2), 142–149. https://doi.org/10.1016/j.gde.2009.02.002
25. Huebner, K., Garrison, P. N., Barnes, L. D., & Croce, C. M. (1998). THE ROLE OF THE FHIT/FRA3B LOCUS IN CANCER. Annual Review of Genetics, 32(1), 7–31. https://doi.org/10.1146/annurev.genet.32.1.7
26. Janssen, A., van der Burg, M., Szuhai, K., Kops, G. J. P. L., & Medema, R. H. (2011). Chromosome Segregation Errors as a Cause of DNA Damage and Structural Chromosome Aberrations. Science, 333(6051), 1895–1898. https://doi.org/10.1126/science.1210214
27. JEPPESEN, C., & NIELSEN, P. E. (1989). Photofootprinting of drug-binding sites-on DNA using diazo- and azido-9-aminoacridine derivatives. European Journal of Biochemistry, 182(2), 437–444. https://doi.org/10.1111/j.1432-1033.1989.tb14850.x
28. Ji, F., Liao, H., Pan, S., Ouyang, L., Jia, F., Fu, Z., Zhang, F., Geng, X., Wang, X., Li, T., Liu, S., Syeda, M. Z., Chen, H., Li, W., Chen, Z., Shen, H., & Ying, S. (2020). Genome-wide high-resolution mapping of mitotic DNA synthesis sites and common fragile sites by direct sequencing. Cell Research, 30(11), 1009–1023. https://doi.org/10.1038/s41422-020-0357-y
29. Kapuściński, J., & Szer, W. (1979). interactions of 4′, 6-diamidine-2-phenylindole with synthetic polynucleotides. Nucleic Acids Research, 6(11), 3519–3534. https://doi.org/10.1093/nar/6.11.3519
30. le Beau, M. (1998). Replication of a common fragile site, FRA3B, occurs late in S phase and is delayed further upon induction: implications for the mechanism of fragile site induction. Human Molecular Genetics, 7(4), 755–761. https://doi.org/10.1093/hmg/7.4.755
31. le Tallec, B., Dutrillaux, B., Lachages, A.-M., Millot, G. A., Brison, O., & Debatisse, M. (2011). Molecular profiling of common fragile sites in human fibroblasts. Nature Structural

& Molecular Biology, 18(12), 1421–1423. https://doi.org/10.1038/nsmb.2155
32. Le Tallec, B., Millot, G. A., Blin, M. E., Brison, O., Dutrillaux, B., & Debatisse, M. (2013). Common Fragile Site Profiling in Epithelial and Erythroid Cells Reveals that Most Recurrent Cancer Deletions Lie in Fragile Sites Hosting Large Genes. Cell Reports, 4(3), 420–428. https://doi.org/10.1016/j.celrep.2013.07.003
33. Letessier, A., Millot, G. A., Koundrioukoff, S., Lachagès, A.-M., Vogt, N., Hansen, R. S., Malfoy, B., Brison, O., & Debatisse, M. (2011). Cell-type-specific replication initiation programs set fragility of the FRA3B fragile site. Nature, 470(7332), 120–123. https://doi.org/10.1038/nature09745
34. Li, S., & Wu, X. (2020). Common fragile sites: protection and repair. Cell & Bioscience, 10(1), 29. https://doi.org/10.1186/s13578-020-00392-5
35. Li, Y., Roberts, N. D., Wala, J. A., Shapira, O., Schumacher, S. E., Kumar, K., Khurana, E., Waszak, S., Korbel, J. O., Haber, J. E., Imielinski, M., Weischenfeldt, J., Beroukhim, R., & Campbell, P. J. (2020). Patterns of somatic structural variation in human cancer genomes. Nature, 578(7793), 112–121. https://doi.org/10.1038/s41586-019-1913-9
36. Limongi, M. Z., Pelliccia, F., & Rocchi, A. (2003). Characterization of the human common fragile site FRA2G. Genomics, 81(2), 93–97. https://doi.org/10.1016/S0888-7543(03)00007-7
37. Lukusa, T., & Fryns, J. P. (2008). Human chromosome fragility. Biochimica et Biophysica Acta (BBA) - Gene Regulatory Mechanisms, 1779(1), 3–16. https://doi.org/10.1016/j.bbagrm.2007.10.005
38. Maccaroni, K., Balzano, E., Mirimao, F., Giunta, S., & Pelliccia, F. (2020). Impaired Replication Timing Promotes Tissue-Specific Expression of Common Fragile Sites. Genes, 11(3), 326. https://doi.org/10.3390/genes11030326
39. Macheret, M., Bhowmick, R., Sobkowiak, K., Padayachy, L., Mailler, J., Hickson, I. D., & Halazonetis, T. D. (2020). High-resolution mapping of mitotic DNA synthesis regions and common fragile sites in the human genome through direct

sequencing. Cell Research, 30(11), 997–1008. https://doi.org/10.1038/s41422-020-0358-x
40. Madireddy, A., Kosiyatrakul, S. T., Boisvert, R. A., Herrera-Moyano, E., García-Rubio, M. L., Gerhardt, J., Vuono, E. A., Owen, N., Yan, Z., Olson, S., Aguilera, A., Howlett, N. G., & Schildkraut, C. L. (2016). FANCD2 Facilitates Replication through Common Fragile Sites. Molecular Cell, 64(2), 388–404. https://doi.org/10.1016/j.molcel.2016.09.017
41. Manzini, G., Xodo, L., Barcellona, M. L., & Quadrifoglio, F. (1985). Interaction of DAPI with double-stranded ribonucleic acids. Nucleic Acids Research, 13(24), 8955–8967. https://doi.org/10.1093/nar/13.24.8955
42. Martin, J. P., & Bell, J. (1943). A PEDIGREE OF MENTAL DEFECT SHOWING SEX-LINKAGE. Journal of Neurology, Neurosurgery & Psychiatry, 6(3–4), 154–157. https://doi.org/10.1136/jnnp.6.3-4.154
43. Minocherhomji, S., Ying, S., Bjerregaard, V. A., Bursomanno, S., Aleliunaite, A., Wu, W., Mankouri, H. W., Shen, H., Liu, Y., & Hickson, I. D. (2015). Replication stress activates DNA repair synthesis in mitosis. Nature, 528(7581), 286–290. https://doi.org/10.1038/nature16139
44. Miron, K., Golan-Lev, T., Dvir, R., Ben-David, E., & Kerem, B. (2015). Oncogenes create a unique landscape of fragile sites. Nature Communications, 6(1), 7094. https://doi.org/10.1038/ncomms8094
45. Mitelman, F., Mertens, F., & Johansson, B. (1997). A breakpoint map of recurrent chromosomal rearrangements in human neoplasia. Nature Genetics, 15(S4), 417–474. https://doi.org/10.1038/ng0497supp-417
46. Murano, I., Kuwano, A., & Kajii, T. (1989). Fibroblast-specific common fragile sites induced by aphidicolin. Human Genetics, 83(1), 45–48. https://doi.org/10.1007/BF00274145
47. Naim, V., & Rosselli, F. (2009). The FANC pathway and BLM collaborate during mitosis to prevent micro-nucleation and chromosome abnormalities. Nature Cell Biology, 11(6), 761–768. https://doi.org/10.1038/ncb1883
48. Naim, V., Wilhelm, T., Debatisse, M., & Rosselli, F. (2013). ERCC1 and MUS81–EME1 promote sister chromatid

separation by processing late replication intermediates at common fragile sites during mitosis. Nature Cell Biology, 15(8), 1008–1015. https://doi.org/10.1038/ncb2793
49. Nalepa, G., & Clapp, D. W. (2018). Fanconi anaemia and cancer: an intricate relationship. Nature Reviews Cancer, 18(3), 168–185. https://doi.org/10.1038/nrc.2017.116
50. OECD Test No (2016). Section 4 in VitroMammalian Chromosomal Aberration Test, OECD Guidelines for the Testing of Chemicals (OECD Publishing). 473.
51. Pelliccia, F., & Rocchi, A. (1986). DAPI-inducible common fragile sites. Cytogenetic and Genome Research, 42(3), 174–176. https://doi.org/10.1159/000132272
52. Pelliccia, F., & Rocchi, A. (1992). The effect of caffeine on DAPI-inducible fragile sites. Mutation Research Letters, 282(1), 43–48. https://doi.org/10.1016/0165-7992(92)90072-P
53. Pelliccia, F., Bosco, N., & Rocchi, A. (2010). Breakages at common fragile sites set boundaries of amplified regions in two leukemia cell lines K562 – Molecular characterization of FRA2H and localization of a new CFS FRA2S. Cancer Letters, 299(1), 37–44. https://doi.org/10.1016/j.canlet.2010.08.001
54. Pelliccia, F., Bosco, N., Curatolo, A., & Rocchi, A. (2008). Replication timing of two human common fragile sites: FRA1H and FRA2G. Cytogenetic and Genome Research, 121(3–4), 196–200. https://doi.org/10.1159/000138885
55. Portugal, J., & Waring, M. J. (1988). Assignment of DNA binding sites for 4′,6-diamidine-2-phenylindole and bisbenzimide (Hoechst 33258). A comparative footprinting study. Biochimica et Biophysica Acta (BBA) - Gene Structure and Expression, 949(2), 158–168. https://doi.org/10.1016/0167-4781(88)90079-6
56. Prantera, G., Cipriani, L., di Castro, M., & Rocchi, A. (1986). Modifications of Human Chromosome Core After Dapi - Undercondensation. Caryologia, 39(1), 33–39. https://doi.org/10.1080/00087114.1986.10797765
57. Prantera, G., di Castro, M., Cipriani, L., & Rocchi, A. (1981). Inhibition of human chromosome condensation induced by

DAPI as related to cell cycle. Experimental Cell Research, 135(1), 63–68. https://doi.org/10.1016/0014-4827(81)90299-8

58. Rocchi, A., & Pelliccia, F. (1988). Synergistic effect of DAPI and thymidylate stress conditions on the induction of common fragile sites. Cytogenetic and Genome Research, 48(1), 51–54. https://doi.org/10.1159/000132585
59. Sarni, D., Sasaki, T., Irony Tur-Sinai, M., Miron, K., Rivera-Mulia, J. C., Magnuson, B., Ljungman, M., Gilbert, D. M., & Kerem, B. (2020). 3D genome organization contributes to genome instability at fragile sites. Nature Communications, 11(1), 3613. https://doi.org/10.1038/s41467-020-17448-2
60. Schwartz, M., Zlotorynski, E., & Kerem, B. (2006). The molecular basis of common and rare fragile sites. Cancer Letters, 232(1), 13–26. https://doi.org/10.1016/j.canlet.2005.07.039
61. Shiraishi, T., Druck, T., Mimori, K., Flomenberg, J., Berk, L., Alder, H., Miller, W., Huebner, K., & Croce, C. M. (2001). Sequence conservation at human and mouse orthologous common fragile regions, FRA3B / FHIT and Fra14A2 / Fhit. Proceedings of the National Academy of Sciences, 98(10), 5722–5727. https://doi.org/10.1073/pnas.091095898
62. Simpson, B. S., Pye, H., & Whitaker, H. C. (2021). The oncological relevance of fragile sites in cancer. Communications Biology, 4(1), 567. https://doi.org/10.1038/s42003-021-02020-5
63. Šípek, A., Mihalová, R., Panczak, A., Hrčková, L., Janashia, M., Kaspříková, N., & Kohoutová, M. (2014). Heterochromatin variants in human karyotypes: a possible association with reproductive failure. Reproductive BioMedicine Online, 29(2), 245–250. https://doi.org/10.1016/j.rbmo.2014.04.021
64. Siri, S. O., Martino, J., & Gottifredi, V. (2021). Structural Chromosome Instability: Types, Origins, Consequences, and Therapeutic Opportunities. Cancers, 13(12), 3056. https://doi.org/10.3390/cancers13123056

65. Smerdon, M. J. (1991). DNA repair and the role of chromatin structure. *Current Opinion in Cell Biology*, *3*(3), 422–428. https://doi.org/10.1016/0955-0674(91)90069-B
66. Smith, D. I., Zhu, Y., McAvoy, S., & Kuhn, R. (2006). Common fragile sites, extremely large genes, neural development and cancer. Cancer Letters, 232(1), 48–57. https://doi.org/10.1016/j.canlet.2005.06.049
67. Soria, G., Polo, S. E., & Almouzni, G. (2012). Prime, Repair, Restore: The Active Role of Chromatin in the DNA Damage Response. *Molecular Cell*, *46*(6), 722–734. https://doi.org/10.1016/j.molcel.2012.06.002
68. Sutherland, G. R. (1977). Fragile Sites on Human Chromosomes: Demonstration of Their Dependence on the Type of Tissue Culture Medium. Science, 197(4300), 265–266. https://doi.org/10.1126/science.877551
69. Sutherland, G. R. (1979). Heritable fragile sites on human chromosomes I. Factors affecting expression in lymphocyte culture. American Journal of Human Genetics, 31(2), 125–135.
70. Tassone, F., & Hagerman, P. J. (2003). Expression of the FMR1 gene. Cytogenetic and Genome Research, 100(1–4), 124–128. https://doi.org/10.1159/000072846
71. Taylor, A. M. R., Rothblum-Oviatt, C., Ellis, N. A., Hickson, I. D., Meyer, S., Crawford, T. O., Smogorzewska, A., Pietrucha, B., Weemases, C., & Stewart G. S., (2019). Chromosome instability syndromes. Nat Rev Dis Primers. 5, 64. https://doi.org/10.1038/s41572-019-0113-0
72. Weise. (2010). Global screening and extended nomenclature for 230 aphidicolin-inducible fragile sites, including 61 yet unreported ones. International Journal of Oncology, 36(4). https://doi.org/10.3892/ijo_00000572
73. Wilhelm, T., Said, M., & Naim, V. (2020). DNA Replication Stress and Chromosomal Instability: Dangerous Liaisons. Genes, 11(6), 642. https://doi.org/10.3390/genes11060642
74. Zlotorynski, E., Rahat, A., Skaug, J., Ben-Porat, N., Ozeri, E., Hershberg, R., Levi, A., Scherer, S. W., Margalit, H., & Kerem, B. (2003). Molecular Basis for Expression of Common and Rare Fragile Sites. Molecular and Cellular

Biology, 23(20), 7143–7151.
https://doi.org/10.1128/MCB.23.20.7143-7151.2003

CONSULTED DATABASES

UCSC Genome Browser Gateway [Human GRCh38p13, Release Data December 2017]:
https://genome-euro.ucsc.edu/cgi-bin/hgGateway?hgsid=281888946_ixUa0qNjLKAtTorOA4GnzFA3aaEG
NCBI Genome Data Viewer [Human GRCh38p13, Release Data May 16, 2021]:
https://www.ncbi.nlm.nih.gov/genome/gdv/
Ensembl [Human GRCh38p13, Release Data August 2021]:
http://www.ensembl.org/Homo_sapiens/Location/Genome
GeneCards [Release Data December 2021]:
https://www.genecards.org/
Mitelmandatabase [Release Data October 2021]:
https://mitelmandatabase.isb-cgc.org/

LIST OF PUBLICATIONS

Balzano E., Di Tommaso E., Antoccia A., Pelliccia F., Giunta S., (2022). Characterization of chromosomal instability in glioblastoma. Frontiers in Genetics, 12:810793. DOI: 10.3389/fgene.2021.810793

Balzano E., Pelliccia F., Giunta S., (2021). Genome (in)stability at tandem repeats. Seminars in Cell & Developmental Biology, 113: 97-112. DOI: 10.1016/j.semcdb.2020.10.003

Balzano E. and Giunta S., (2020). Centromeres under pressure: Evolutionary innovation in conflict with conserved function. Genes (Basel), 11(8): 912. DOI: 10.3390/genes11080912

Maccaroni K., **Balzano E.**, Mirimao F., Giunta S., Pelliccia F., (2020). Impaired Replication Timing Promotes Tissue-Specific Expression of Common Fragile Sites. Genes (Basel), 11(3):326. DOI: 10.3390/genes11030326